Effect of ink composition on the physical characteristics and performance of aerosol jet printed lithium cobalt oxide cathodes

THESIS

Amber Powell

AFIT-ENP-MS-20-M-114

DEPARTMENT OF THE AIR FORCE
AIR UNIVERSITY

AIR FORCE INSTITUTE OF TECHNOLOGY

Wright-Patterson Air Force Base, Ohio

AFIT-ENP-MS-20-M-114

Effect of ink composition on the physical characteristics and performance of aerosol jet printed lithium cobalt oxide cathodes

THESIS

Presented to the Faculty

Department of Physics

Graduate School of Engineering and Management

Air Force Institute of Technology

Air University

Air Education and Training Command

In Partial Fulfillment of the Requirements for the

Degree of Master of Science in Materials Science

Amber S. Powell, BS

March 2020

AFIT-ENP-MS-20-M-114

Effect of ink composition on the physical characteristics and performance of aerosol jet printed lithium cobalt oxide cathodes

Amber S. Powell, BS

Committee Membership:

Maj Nicholas Herr, PhD
Chair

Dr. Larry Burggraf
Member

Dr. Thomas Howell
Member

AFIT-ENP-MS-20-M-114

Abstract

Nine ink compositions were formulated and printed utilizing aerosol jet printing to form lithium cobalt oxide battery cathodes. This fabrication method is being investigated to determine the viability and potential benefit of aerosol jet printing for unique parts where a flat dense cathode would be undesirable. The conditions for creating the ink and printing of the tapes were held constant. The inks and resulting cathode tapes were characterized utilizing TGA, SEM, and electrochemical testing to observe the effect of ink composition on the surface roughness and electrochemical properties of the cathode tapes. The printed tapes had unique surface features that seemed to be ink dependent. This resulted in less dense tapes than the tape cast cathodes. Many of the tapes had a higher specific capacity when compared to similar tape cast materials. These results show this to be a viable fabrication method for lithium cobalt oxide cathodes and further investigation would be encouraged.

Acknowledgments

I would like to express my sincere appreciation to my faculty advisor, Major Nicholas Herr, for his guidance and support throughout the course of this thesis effort. I would, also, like to thank my mentor, Dr. Thomas Howell, with the Air Force Research Laboratories for both the opportunity to work on this material and the support shown throughout the process. Finally, I would like to thank Thomas Jenkins who taught me everything I needed to know to get started in the labs and helped me make my first battery.

Amber S. Powell

Table of Contents

Page

List of Figures

Page

List of Tables

Page

Effect of ink composition on the physical characteristics and performance of aerosol jet printed lithium cobalt oxide cathodes

I. Introduction

General Issue

The more we can advance energy storage technology the further we can distance ourselves from outdated and environmentally unfriendly technologies. The current methods for formulating batteries are limited. Currently cathode tapes are made in sheets that must be manipulated into new shapes and forms to fit into predetermined battery casings. The tape casting method used most prominently allows for limited control on the thickness or microstructure of the final product. It must be applied to a flat substrate without exceptions. Printing allows for an alternative to this method through control of a multi-axis stage and programming software.

A new printing method has the potential to tailor batteries for new applications. Currently micro batteries use thin film cathodes to reduce the battery's size as much as possible however this limits the energy density of the cathodes. A 3D structure within the individual layers can maximize the usable surface area which leads to an increase in the energy density as demonstrated in several research scenarios described below. This structured battery could be the avenue to making more powerful micro batteries that allow us longer battery life or smaller devices. These micro-sized structures have only been achieved through high precision printing processes.

On a larger scale, current battery packs for UAVs or electric cars are rather bulky and any weight or space savings significantly improves the performance. A printing method that can deposit battery materials onto curved surfaces, thereby integrating the battery

technology into the vehicle's body by replacing the typical plastic or metal structural components of the vehicle, would remove the need for the bulky batteries and allow for considerable weight savings.

In addition to the reasons listed above printing allows for high throughput and reduces human error by automating the processes. Promising results have been shown for printing all parts of the battery just by switching out the ink which reduces the number of steps required when assembling the battery. Aerosol jet printing technology is utilized for coatings and solid oxide fuel cells in automotive and aerospace industry. These fields will provide a template for scaling up aerosol jet printing in the battery industry. Additional research and testing will be required to fully understand how the battery materials are affected by this process.

Research Objectives

The primary objective of this research is to show aerosol jet printing can produce a $LiCoO_2$ cathode with a high specific capacity. The electrochemical properties of these batteries will be measured and compared to tape cast batteries to determine the viability of this method. It is expected by holding printing conditions constant, inks, printed with aerosol jet printing, will exhibit surface features that affect their electrochemical properties by exposing more surface area.

The ink compositions of these cathodes will be varied with respect to solid composition (binder, carbon, and $LiCoO_2$) and weight percent solids in the ink to observe the effect of different inks on the surface morphology formed during printing. Printing conditions will be held constant to evaluate the effect of the ink composition on both the

electrochemical performance and surface morphology of the resulting tape. Secondary electron microscopy will be utilized to observe the features formed after printing and drying. It is believed different rheological properties of the ink will result in a variety of sizes and shapes in the surface features which will present different amounts of porosity to the electrolyte. An increase in porosity resulting in more exposed surface area is expected to result in a higher specific capacity due to more accessible $LiCoO_2$.

Methodology

Jay Denier et. al. was able to successfully print a thick, 170 µm lithium iron phosphate ($LiFePO_4$) cathode with a discharge capacity of 151 $mAhg^{-1}$ at a C/15 rate (~88% of the theoretical 170 $mAhg^{-1}$) which maintained 89% of this value after testing for 50 cycles at various rates [1]. With this proof of concept, high functioning $LiCoO_2$ cathode printing should be possible, although only thin $LiCoO_2$ cathodes had been printed within the laboratory at Air Force Research Laboratory (AFRL). These thin cathodes exhibited poor performance, less than 80% capacity on the first cycle. Through a weight loss study of these cathodes it was found only a fraction of the $LiCoO_2$ that was in the ink was printed and ended up in the final tape. This resulted in inaccurate calculations of the maximum capacity and C rate for the printed cathodes, skewing the specific capacity measurements.

If the inks are not stable during printing, settling will occur and the ink droplets that aerosolize will have an undesirable ratio of materials, higher solvent content and less active material. Based on the weight loss study and the performance of these batteries it is possible this was occurring in the early printed batteries. Comparing the two lithium

materials, the most discernable difference is their particle size and shape. The $LiFePO_4$ particles are much smaller and more spherical than the $LiCoO_2$ particles making them easier to suspend in a low viscosity ink. Utilizing Deiner's ink design and reducing the particle size of the $LiCoO_2$ allowed for creation of a stable ink that was able to print relatively thick cathodes. Thicknesses printed with the inks in this paper ranged from 40 – 120 µm. Many of these resulting tapes performed better than previously printed tapes. This study shows many of these printed cathodes achieved up to 97% of the specific capacity for $LiCoO_2$ cathodes. These values were compared to $LiCoO_2$ cathodes that were tape cast in the laboratory and achieved up to 93% capacity. The microstructure of the printed cathode was examined to determine a cause of the increase in specific capacity.

Denier observed features on the surface of the printed cathode tapes that created a system of interconnected porosity throughout the cathode. These features contribute to an increase in surface area through which the lithium ions can diffuse into the electrolyte and may provide access to active material that is otherwise unavailable to a tape with a higher bulk density, such as the tape cast cathodes. These features are also observed in the $LiCoO_2$ prints. Denier was unable to discover a reason for the formation of these features. Having control over these features would be beneficial to control the porosity and surface area exposed to the electrolyte. Porosity and thickness in tape cast cathodes can be controlled by varying the particle size and rheology of the slurry so this study was created to investigate the effect of ink composition on the surface features formed through printing. By changing the solid composition (binder, carbon, and LiCoO2) and weight percent solids in the inks printing will be performed on a variety of inks with different rheological properties.

A Brief History

A battery in this context is a device made of one or more cells that store chemical energy to be released in an electrical form. The first battery capable of producing current for an extended period of time, up to 1 hour, was created so Alessandro Volta could prove electricity can be generated from inorganic materials, copper and zinc in this initial case. Prior theories believed organic materials were the source of electricity. For Volta's battery, the two dissimilar metals were stacked together with a thin, salt water soaked, piece of cardboard between the metals. By attaching an external circuit, the chemical potential difference in the two metals forces electrons and ions to flow until the chemical potentials are equivalent. The details of this reaction will be described later within this paper as well as the many issues with this early battery. The ability to produce a steady current was previously considered impossible and led to the discovery of water electrolysis as well as Faraday's study of electromagnetism. However, these early batteries are clearly not sufficient for modern needs such as cell phones, drones, and electric cars. [2]

Current Needs

Batteries are essential in modern life; they power our cell phones, portable tablets, and electric vehicles which are replacing gas vehicles on the road as well as in the skies. Creating smaller, more energy dense batteries will allow technology to advance by making smaller, lighter devices with longer use time between charges.

Solar and wind power are great alternatives to fossil fuels as we try to reduce our carbon foot print to zero. One of the downsides to these energy sources is that the energy

produced cannot be controlled to meet day to day demand like fossil fuels are. If the sun is not shining or the wind is not blowing then no energy will be produced and any excess energy that is produced will need to be stored and reserved. This shift to renewable resources requires larger more efficient batteries capable of storing enough energy to power a community. Increasing the scale and production capabilities currently in place as well as designing new manufacturing methods and better materials will allow us to meet the increasing demand. 3D and jet printing are technologies that have been implemented in other high production technologies such as fuel cells and automotive coatings. The research into printing for batteries applications is just getting underway.

Portable electronics are heavily reliant on battery technology. These devices continue to decrease in size and increase in processing power, as predicted by Moore's law. As processing power increases in these small devices, the energy requirements continue to increase calling for more energy dense materials. To create some of the technology depicted in science fiction, such as projection wrist watches or micro-sized phones the batteries will need to support the amount of power required to run these devices for an average work day in a very limited space. There are a limited number of ways to increase the energy density of a battery without moving to new materials and a new chemistry. One way is to reduce the size and remove the need for stacking of the components as will be explained later. The current methods of manufacturing batteries cannot accommodate this but an automated high precision printing system may allow for increased performance of the materials we are most familiar with.

Military equipment is also making advancements to allow military missions to be safer and easier for the soldiers in the field. Unmanned air vehicles (UAVs) are a current

field of interest. The farther they can travel on a single charge; the more information can be gained. Currently, a large and bulky battery pack is placed in a battery bay, and limits the space available for additional equipment on board. The battery plus the structural frame of the UAV adds up to a large amount of weight and space. If batteries could be made more structurally functional it would be possible to replace portions of the UAV body with multifunctional battery materials and to provide a considerable weight savings. This battery material would need to provide a stiffening mechanism for various parts and perform well under standard aerospace mechanical testing and cycling while maintaining its electrochemical performance. One step in this would be depositing battery materials onto curved and complex surfaces rather than the flat panels that are generally produced. Fabrication methods must also offer dimensional control across the micro and meso length scales. This same benefit could be realized in the automotive industry with the manufacturing of electric vehicles.

II. Background

Chapter Overview

The purpose of this chapter is to provide relevant background material on battery chemistries and processing that will benefit the reader for the remainder of the paper.

Battery Basics

Batteries are defined as a device that converts chemical energy stored in active materials into electrical energy by way of oxidation-reduction (redox) reactions [3]. Batteries transfer their stored energy when a circuit is completed between the positive and negative terminals. If they are not connected to a circuit the battery should remain inert. Any reactions that occur while the battery is not in use will degrade the quality of the battery. When the circuit is completed and the battery is connected to a device that requires power an oxidation reaction occurs at the anode which is comprised of a material that will easily give up its electrons to a negative terminal. The resulting ion passes through the electrolyte to the cathode, leaving a vacancy in the anode material. The cathode accepts electrons from the positive battery terminal completing the circuit and allowing electricity to flow. This process continues until there is no longer a difference in the chemical potentials of the cathode and anode [4] The anode and cathode within a battery are separated by a material that conducts ions but not electrons. This forces the electrons to flow into the connected device until the battery is depleted. Referring back to the Voltaic stack, an example of the redox reactions and the corresponding potential energy produced is shown in equations 1-3.

Cathode: $Zn(s) \rightarrow Zn^{+2}(aq) + 2e^{-}$	-0.76V	(1)
Anode: $\boldsymbol{Cu^{+2}(aq) + 2e^{-} \rightarrow Cu(s)}$	+0.34V	(2)
Total: $Zn(s) + Cu^{+2}(aq) \rightarrow Zn^{+2}(aq) + Cu(s)$	+1.10V	(3)

This reaction is a simplified version of what is actually happening within a Voltaic stack, and when compared to modern batteries is inefficient. The salt water, used as the electrolyte, reacts with the copper metal producing hydrogen gas which is not only dangerous but the energy used in this side reaction is subtracted from the total energy the battery can supply. It is important to remember reactions such as these when selecting materials. Each component of the battery must be stable until the circuit is completed and then only the desired reactions should be allowed to proceed. This selection process is made difficult because most materials that make good batteries, such as lithium, are highly reactive in oxygen and water. This constrains the production process and can limit its shelf life. The production environment and purity of the materials can have a large effect on battery quality as will be discussed later in this paper.

The amount of energy produced in a standard redox reaction is referred to as the standard Gibbs Free Energy. This energy is material dependent resulting from the chemical potential difference between the two materials. The total energy produced during this reaction can be calculated using the energy produced by the two half reactions. In batteries this potential difference is the amount of work available to push the charge through the circuit. Values for the individual materials are determined experimentally and can be found in most chemistry text books.

Rechargeable Batteries

Most chemical batteries, including the Voltaic stack, are primary batteries, meaning the reaction will only progress in one direction and cannot be reversed due to the chemical break down of the materials. Once the materials have given up their energy and reached an equilibrium, they are no longer useful. Most battery materials fall into this category. After a single use these batteries are disposed of producing large amounts of hazardous waste. It would be ideal to replace these types of batteries and especially batteries that require larger amounts of current with something that can be reused.

Certain battery chemistries maintain their structure during the discharging process, allowing the reaction to be reversible. These batteries, called secondary batteries, are rechargeable and include lead-acid car batteries and lithium ion batteries. The electrodes in rechargeable batteries have a structure that allows the ions to travel into and out of both the anode and cathode without a loss of structural and chemical integrity over a specific, material dependent, voltage range. This occurs through a process called intercalating, where the ions insert themselves into the structure of the electrodes [5]. Once a certain percentage of the ions have moved from the anode to the cathode the process is then reversed.

The capacity of a battery is the measurement of energy that can be stored by the battery. The theoretical capacity is based on the weight of the active materials anticipating 1 mol equivalent of active material will deliver 26.8 Ah [4] The theoretical capacity of a battery may be calculated in units of A*hr/g using Faraday's law, as seen in equation 4, where n is the number of charge carriers in, F is Faraday's constant (26.8 hr*A/mol), and g is the molecular weight of the active material in the electrode.

$$Q_{theoretical} = \frac{nF}{g} \quad [4]$$

The capacity calculated above is much higher than a rechargeable battery can hold and remain stable. The reaction that occurs in reversible batteries results in an ion migrating from one material to another and therefore cannot be taken to completion. At a certain amount of ion depletion, permanent defects will form causing the structure of the material to break down due to unwanted reactions. This occurs at a percentage of the theoretical capacity. The actual capacity of the battery is directly related to the number of ions lost from the electrode. If too many ions are removed from the electrode there will not be enough remaining to maintain the crystal structure of the material.

The reaction that takes place in a rechargeable battery is stable over a limited voltage range that can be determined through cyclic voltammetry, a process where the potential voltage is ramped linearly over a set time. The rate of current change is then measured to determine when oxidation or reduction reactions are taking place in both the forward and reverse reactions, in the anodic and cathodic traces. This test provides data on the potential value at which certain reactions will occur and the rate at which they occur as shown in **Figure 1**. This data can also be utilized to determine the reversibility of the reaction by measuring the distance between the anodic and cathodic peaks. This test is used to determine if the materials are stable over the voltage range tested. The amount of capacity that is usable is material dependent, for $LiCoO_2$ this occurs at ~50% lithium ion depletion as shown in **Figure 1**. Utilizing more of this capacity would begin to degrade the materials. If the reaction is taken too far unwanted reactions may occur between the electrode and electrolyte forming products that will limit the movement of

electrons or ions and thus increase the resistance of the battery [6]. The graph in **Figure 1** takes the reaction past its stability point and a phase change from a hexagonal to a monoclinic crystal structure will occur in the $LiCoO_2$ at higher voltages. This phase change limits the reversibility of the cell [7]. The same test for Lithium Nickel Cobalt Manganese Oxide (NCM) and a Lithium Iron Manganese Cobalt Phosphate (LFMCP) material was performed and is graphed in **Figure 1** as an example of the unique voltammograms different materials will create. The NCM and LFMCP materials are mixtures of lithium ion cathode materials. These materials are being researched as a way to lower the amount of high priced $LiCoO_2$ required in the cathode, while maintaining a large stable voltage range.

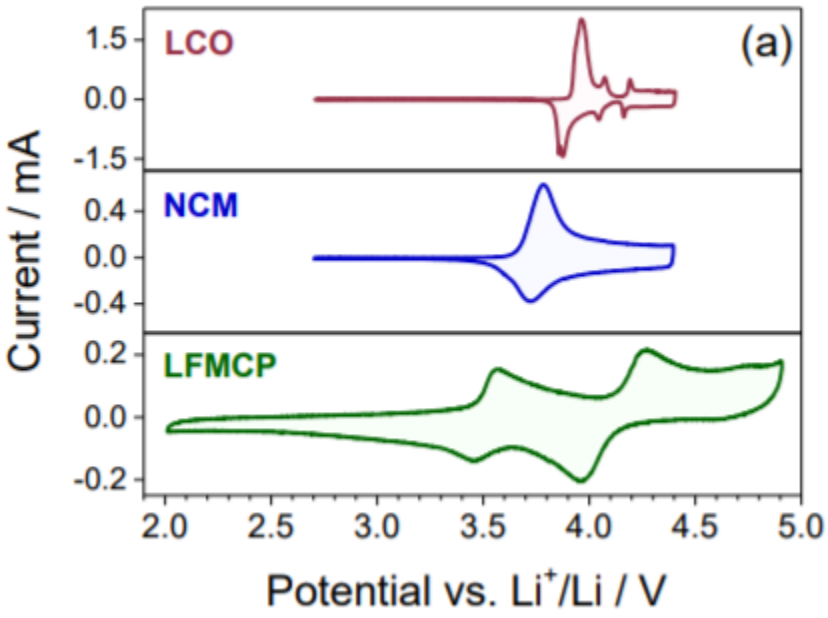

Figure 1. Cyclic voltammetry of $LiCoO_2$, NCM, and LFMCP battery materials. The cathodic trace on the positive side of the graph and describes the reduction of the cathode and the negative part of the graph is the anodic trace that describes the oxidation. The peaks indicate different oxidation states. **[7]**

Impedance is a combination of internal resistance and reactance. Electrical impedance tests are utilized to determine the resistance within the battery. These tests load the battery with a specific AC potential (amplitude) over a range of frequencies (typically 1 MHz to 1 Hz) sine current and measures the corresponding voltage response to create a Nyquist plot with the x-axis as Z' representing the resistance elements and the y-axis as Z" representing the reactance. Batteries must consider both the electronic energy flow and the ionic movement. The measurements made at different frequencies will relate to different electronic or ionic movement within the battery. Higher frequency measures inductance and ohmic resistance of the battery. As the frequency is decreased the resistance due to the charge transfer reaction at the electrode surface can be extrapolated and finally at the lowest frequencies the diffusion resistance can be described using a Warburg element [8]. The lower the resistance, generally, the higher the capacity of the battery. Any increase in resistance can lead to reduced electron or ion pathways slowing the flow. Typically, all batteries will have some increase in resistance over time as the battery is cycled due to a resistive layer that will build up at a very slow rate.

A full charge and discharge (over the voltage range in which the batteries are stable) is called a cycle. Rechargeable batteries may be cycled multiple times, however, because no reaction is ideal the battery still degrades over time. The number of charge and discharge cycles a battery can perform before it is reduced to 80% of its theoretical capacity is referred to as a batteries cycle life. The rate of the charging and discharging of the battery is given as a C-rate. This is calculated by C/x where C is the capacity of the battery materials and x is the number of hours it should theoretically take to completely

charge or discharge the battery. The actual capacity of the battery can be determined by the time taken to complete one cycle. A common and simple method of charging/discharging is constant current (CC) where the battery is charged/discharged at a constant current while measuring the voltage response, until it reaches the set voltage limit. Testing can occur over a constant applied voltage. Sometimes a mixture of these two charging methods is utilized to ensure full capacity is reached without over charging the battery. The method discussed within this paper is performed with a constant current during charge and discharge [4]. The rate at which the battery is cycled will affect the actual capacity. In the same way chemical reactions are rate dependent, the slower a battery is discharged the higher the capacity, or number of ions transferred, will be. An increased charge or discharge rate can degrade the battery over time.

As the ions are moving back and forth the terms cathode and anode become interchangeable. For the purposes of this paper the negatively charged electrode when the cell is discharging will be referred to as the anode (for example lithium metal).

Lithium Ion Batteries

The first rechargeable lithium ion battery (LIB) was designed almost 40 years ago by John Goodenough, Rachid Yazami, and Akira Yoshino. They received many awards for this achievement including the IEEE Medal for Environmental and Safety Technologies in 2012 and the Nobel Prize for Chemistry in 2019. LIBs were first mass produced by the Sony Corporation in 1991 as a replacement for Moli Energy Lithium/MoS_2 batteries which had begun catching fire and causing injury to users of Sony devices. Today lithium ion batteries are used in phones and electric cars. Lithium is the lightest metal and

therefore has the highest specific energy density of any of the elements. The small size of the lithium ion allows it to be easily transported through the electrolyte and separator with little damage to the surrounding electrode materials, a schematic can be seen in **Figure 2**. The energy required to ionize lithium metal is comparatively low and it possesses the highest theoretical capacity of any material. Lithium's highly reactive nature makes it an excellent battery material when considering efficiency but does create a safety concern [9].

Utilizing lithium metal as the anode material is extremely efficient and provides high specific capacities for the first several cycles of a battery's life. However, the metal creates a dendritic phase when the batteries are cycled multiple times. This phase can pierce through the electrolyte layer creating an internal short [3, 9]. Lithium metal is also highly reactive to water and air so it must be handled with care. In lieu of finding a method to prevent this dendritic growth, graphite has been used in place of the lithium metal as a more stable anode material. This comes with its own difficulties that will be discussed further below. LIB cathodes are made of lithium-based oxides with transition metals, including cobalt, nickel, magnesium, exc. These transition metals can be expensive due to the rarity. That being said few chemistries have been able to compete with the performance and price of the lithium ion battery and research is ongoing to improve upon it.

There is a growing demand for LIBs with higher capacities, faster charge-discharge rates, and lower cost to be used in new and more demanding environments. Research to address these needs have been investigating novel battery materials, architectures and, as is the focus of this paper, new fabrication methods [6].

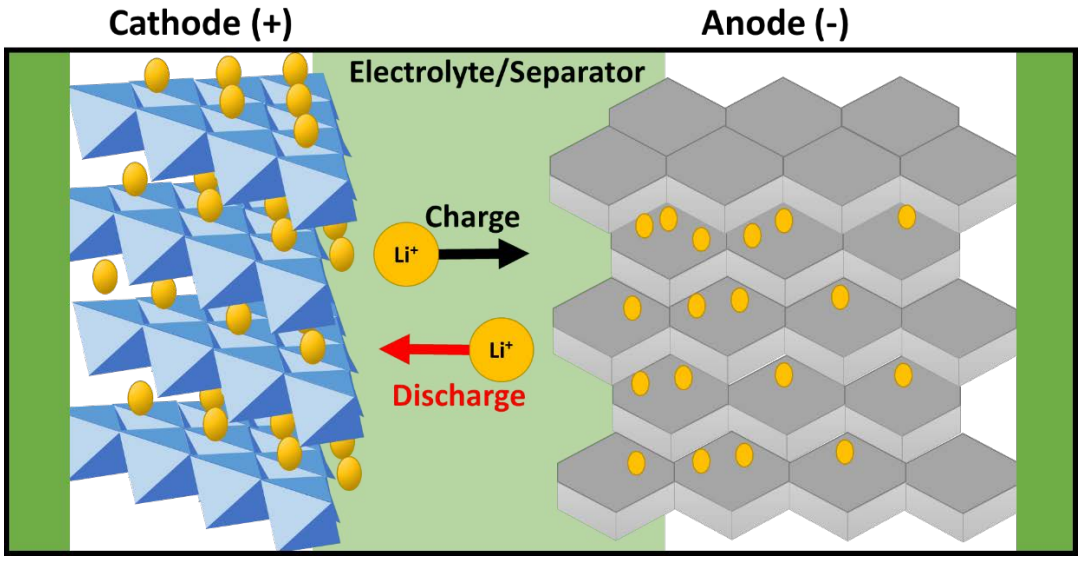

Figure 2. Lithium ion battery with a transition metal oxide cathode and a graphite anode.

Electrochemistry

In the case of lithium ion batteries, specifically a lithium cobalt oxide cathode and a lithium metal anode the lithium ions are transported through the electrolyte, oxidizing the cobalt metal from Co^{+4} and Co^{+3} during the discharging phase. For lithium ion batteries degradation begins when approximately 50% of the lithium is removed. Past this point Li_2O, CoO, or O_2 gas may form causing volume and pressure changes within the cell. To prevent this formation the batteries are cycled between 3.0V to 4.2 V and the resulting reactions can be seen in equations 5, 6, and 7. Charging above 4.7V causes an irreversible phase transition in the CoO_2 from hexagonal to spinel [10]. Methods to improve upon this capacity range are being researched through coating the surface of the electrode with ZnO or polymers [11, 12].

Cathode: $\mathrm{Li_{1-x}CoO_2 + xLi \leftrightarrow LiCoO_2} \quad E^{\circ}_{1/2} = 4.2V$ (5)

Anode: $\mathrm{Li \leftrightarrow Li^+ + e^-} \qquad E^{\circ}_{1/2} = 3.045V$ (6)

Total: $\mathbf{LiCoO_2 + Li^+ + e^- \leftrightarrow LiCoO_2} \quad \boldsymbol{E^{\circ}_{cell} = 1.955V}$ (7)

Using equation 4 the theoretical capacity of lithium metal can be calculated. Lithium has a molar weight of 6.94 g/mol and contributes 1 electron and therefore has a theoretical capacity of 3,850 mAh/g. Lithium cobalt oxide ($LiCoO_2$) has a molecular weight of 97.87 g/mol which results in one of the highest theoretical capacities of the lithium oxide materials, 273 mAh/g, and is the most widely used of the lithium ion cathode materials [3]. To prevent cell degradation $LiCoO_2$ batteries with a lithium metal anode are cycled and the total capacity is measured against about half of this theoretical capacity, 140 mAh/g which relates to about half of a mole of lithium ions.

Anode Materials

The primary purpose of the anode is to plate or intercalate the ions coming from the cathode within the anode material and to give them back up when charging. For lithium ion batteries, lithium is a preferred anode material for the reasons discussed above but over the batteries lifetime the cycling process causes dendrites to form on the surface of the metal as the lithium ions plate onto the anode. This phase grows into long sharp crystals which may pierce the separating layers to reach the cathode which will cause a short. A short occurs when a shorter conductive path for the electrons to reach the cathode is presented. This results in the electrons taking the shorter path rather than traveling through the connected device and causes negative voltage spikes, thermal runaway (where the temperature increases exponentially) and finally, the battery has the

potential to explode. Anode coatings and solid-state electrolytes are currently being studied as ways to prevent the dendritic growth from leading to catastrophic failure.

Graphite is used as a safer alternative to lithium metal that many companies have switched to but research is ongoing to perfect this anode material. Processing can be difficult because the solvent used when making the graphite electrode co-intercalates with the carbon disrupting the structure formed. This creates blocked areas which the ions cannot travel through easily [9]. The electrolyte has a tendency to react with the carbon as the battery is cycled forming a solid electrolyte interphase (SEI) layer with high resistivity over the life of the battery. The resistive layer will prevent ions from passing through. Both are less catastrophic failures than the failures that can occur with lithium metal but detract from the overall performance. Yoshino has performed extensive work with additives to address the problems with the carbon anode and also with the electrolyte to find a salt that would be the least reactive.

While generally less safe, lithium is a well-studied material that produces good results when used for short periods of time and was determined to be the best material for testing batteries in this study.

Electrolyte Materials

Electrolytes in lithium ion batteries are typically lithium salts dissolved in non-aqueous carbonated organic solvents. Organic solvents are non-polar molecules that have low dielectric constants. This limits the solubility of the salts which causes low conductivity (0.01-0.001 Scm-1) and limits the stability at high voltages (>4.6V). [4]

As long as the voltage stays within the stable range, the electrolyte does not take place in the reaction, it instead acts as a medium for the ions to move through while preventing electrons from passing.

Liquid electrolyte is soaked into a porous separator material, often glass fiber, which ensures the anode and cathode do not touch while keeping the electrolyte in contact with both electrodes. The battery materials are then sandwiched together and are often compressed to ensure good contact. The closer the cathode and anode are to one another the shorter the distance the ions have to travel which is beneficial because non-aqueous electrolytes have relatively low ionic conductivities. [4] LIBs have been limited to thin electrodes (20-100 μms) with simple shapes (e.g. coin, cylinder, prismatic, and pouch cells). To meet the current energy needs these limits are being explored and expanded on. [13]

Higher contact of the electrolyte with the electrodes through increased surface area will allow for a shorter pathway for the electrons to travel. Reactions take place at the surface; therefore small particles with high surface area in which good contact with the electrolyte can be sustained is preferred. At some point the particle size is small enough to make unwanted reactions between the active material and the electrolyte favorable. Ion movement in this case will be difficult, or become increasingly more difficult, as the products of these unwanted reactions create a barrier. There is a balance between these reactions that must be maintained.

In the case of liquid electrolytes, it is important that the electrolyte wets the surface of the batteries and is able to penetrate into the material. This can be increased by creating large geometric electrode areas and tortuous porosity in the cathode [9]. Solid

state electrolytes, which includes gel, polymer, and ceramic materials, are being looked at as a more structurally stable and less reactive electrolyte. Solid state batteries provide a pathway for utilizing lithium metal anodes while minimizing the reduction in cycle life commonly seen in this material due to dendrite formation. The dendrites are unable to pierce the solid electrolyte. These solid electrolytes are typically more resistive than liquid electrolytes at room temperature. The electrolyte efficiency increases as they are heated to higher temperatures as the ion movement at higher temperatures is improved. The reactivity is also increased at these higher temperatures which can have a negative impact specifically on the liquid electrolyte.

Issues with electrode contact arises with solid state electrolytes. These electrolytes are typically cast separately from the electrodes and must be sandwiched together using mechanical pressure applied through methods such as calendaring. Calendaring is a process where a tape like material is passed through rollers at high pressure to produce a smooth material with a reduced thickness and increased bulk density. In this case the pressure is used to create contact between the electrode and electrolyte. Without this contact the ions cannot be transferred between the electrodes. Research is ongoing into printing methods that create 3D architectures that allow the electrolyte to be printed into a 3D electrode structure insuring maximum contact as shown in **Figure 3** [13]. These structures are ideal for micro-type batteries where thin electrodes are required [14].

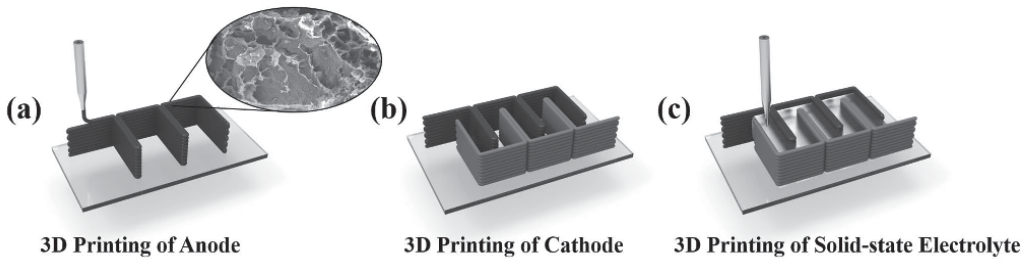

Figure 3. 3D printed electrodes and solid-state electrolyte. **[15]**

Cathode Materials for Lithium Ion Batteries

Active Materials

The active materials in a lithium ion battery cathode are lithium-based oxides with transition metals that undergo oxidation to higher valence states when the lithium is removed. Common lithium ion cathodes utilize $LiCoO_2$, $LiMn_2O_4$, $LiFePO_4$ and $LiFeSO_4F$. Each of these has a different crystal structure that acts as the scaffolding to transport the lithium ions within the material as shown in **Figure 4**. Olivine structures such as $LiFePO_4$ have particles that tend to take a spherical shape while layered structures such as $LiCoO_2$ take on non-spherical plate-like shapes. **Figure 5** shows typical voltage discharge profiles for some of these cathode materials. Not only do the crystal structures effect the shape of the particles in the battery but also the ability of the lithium ions to move through the material on its path to reach the electrolyte. $LiCoO_2$ has planes of CoO_6 through which the lithium ions move when delithiation and lithiation takes place. New materials have been created by substituting a percentage of the cobalt with nickel, manganese, aluminum or iron to lower the price of the active material and hopefully maintain or improve upon the properties from the cobalt [14].

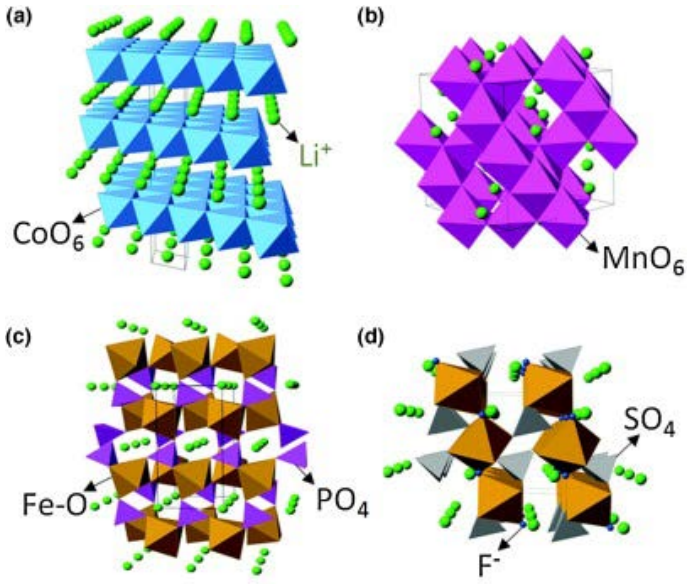

Figure 4. Representative crystal structures of cathode materials for lithium-ion batteries: (a) layered α-$LiCoO_2$; (b) cubic $LiMn_2O_4$ spinel; (c) olivine-structured $LiFePO_4$; (d) β_{II}-Li_2FeSiO_4; and (e) tavorite-type $LiFeSO_4F$. Li ions are shown as light green spheres, CoO_6 octahedra in blue; MnO_6 octahedra in mauve, Fe–O polyhedra in brown, PO_4 tetrahedra in purple, SiO_4 tetrahedra in light brown, SO_4 tetrahedra in grey, and in (e) fluoride ions in dark blue. Black lines demarcate one-unit cell in each structure. **[16]**

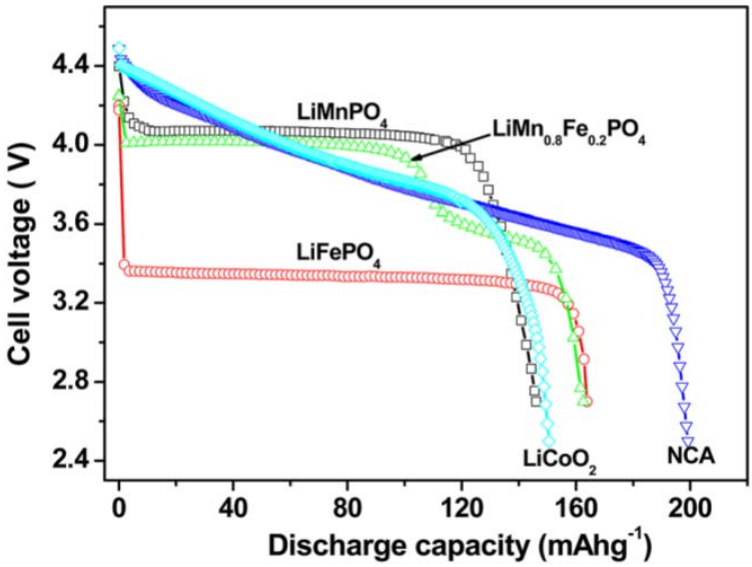

Figure 5. Typical voltage profiles of olivine $LiFePO_4$, $LiMnPO_4$, and $LiMn_{0.8}Fe_{0.2}PO_4$, and layered $LiCoO_2$, $LiNi_{0.8}Co_{0.15}Al_{0.05}O_2$ (NCA) cathodes, measured in galvanostatic measurements in EC-PC/LiPF6 liquid electrolyte solutions at C/20 rates. **[16]**

Intercalation and deintercalation occur along specific crystallographic planes and higher crystallinity improves electrode performance. The reaction occurs at the surface of the electrode so small particles with high surface area are typically preferred. Smaller particles have other issues such as agglomeration and high reactivity that is undesired so often intermediate size particles are selected for the ease of processing. A certain amount of porosity is required in the electrode to allow the electrolyte to penetrate into the cathode and it has been shown porous active material particles can also perform better than nano-particles which will typically form a very dense cathode [14].

Non-active Cathode Materials

The active materials must be electrically conductive; however, this is limited at particle interfaces and grain boundaries. Conductive materials such as carbon black and graphite are typically added to increase the electrical conductivity. It is important for the conductive carbons to have good contact with all of the particles of active material. If active material is cut off from the conductive portions they will not be fully utilized and will contribute no ions, lowering the cell capacity [9].

A binding material is utilized to hold the active materials and carbon in place and to ensure it sticks to the current collector. This binder must be electrically conductive or it will increase the resistivity of the cathode. Polyvinylidene di-fluoride (PVDF) is a semi-crystalline polymer commonly used as a binder in battery materials due to its electrical conductivity (maximum of ~10^{-2} S/m [9]). PVDF will dissolve in many non-aqueous solvents when heated and undergoes swelling in certain solvents at room temperature [17]. The flexibility allowed by this polymer helps relieve stresses formed when the active material undergoes volume changes [9].

Both materials are added weight that do not contribute to the formation of lithium ions and therefore the amount added should be minimized to maximize the specific energy density of the cell. The percentage may be chosen as a way to control the physical characteristics of the tape. Higher percentages of carbon or binder will increase the viscosity which may lead to increased porosity or more shrinkage when tape casting. The ratio of these components will affect the cyclability and rate capability of the battery. The electrical and physical properties will both be affected by the amount of additives used so the end use of the battery should be considered when choosing the composition of the cathode.

In addition to the required components in the cathode, anode, and electrolyte the total weight of the battery must also consider components such as current collectors and the casing. The more "inactive" material that is added the lower the overall energy density will be.

Current Collector Materials

The current collector directly supports the active materials and provides a pathway for charge to flow into and out of the active materials. To aid in this it must be stable within the operating voltage to prevent corrosion and compatible with the active materials. If the electrodes delaminate electron flow will be halted so maintaining good adhesion is key. For lithium ion batteries thin (15-20 μm), flexible metal foils of aluminum or copper are used for the cathode and anode respectively. The foils are thin to reduce the added mass and provides the added benefit of flexibility. Good adhesion between the foils and the electrodes is required so they can withstand some flexing without delaminating [4]. Carbon coating these foils has shown to improve adhesion and

conductivity. For some applications a flexible battery may be required however the mechanical stress will degrade the battery performance.

Battery Casing Materials

The casing must contain the battery materials, preventing air and moisture from reaching the active materials, and be chemically resistant to the products formed during the battery cycling. Often this is a thin aluminum metal laminated with a nonreactive plastic. During the early cycling gases may be produced that form pressure inside the battery case. The size and thickness of the active materials will affect the amount produced. If too much gas is formed additional safety measures may be required but this is typically not necessary for thin film batteries [4]. The casing must be sealed with pressure or heat. The use of the battery determines what shape the case may take but common examples are pouch or coin cells.

Fabrication Methods for Lithium Ion Batteries

This paper is concerned with the viability of a new printing method. This section covers the methods that are currently being utilized. This consists mainly of tape casting with some niche uses of flexographic printing.

The most commonly used technique for fabricating cathodes is tape casting as seen in **Figure 6**. The equipment ranges from small hand held doctor blades used in labs to large automated reel to reel systems to create production quality cathodes. The blade is set to certain height from the substrate to control the thickness. The blade height is typically set between 50-200 μm for controllable results. The substrate consists of the thin metal foil current collectors. A viscous slurry is pooled below the blade which is then

drawn at a constant speed over the wet material which is forced through the gap producing a thin uniform coating on the substrate. The speed the doctor blade is moved as well as the rheology and composition of the slurry effect the final product. This process is limited as it cannot produce unique geometries or patterning, if this is required it must be added in a post processing step. To create the different battery geometries, shapes are cut from the flat cathode tape [4].

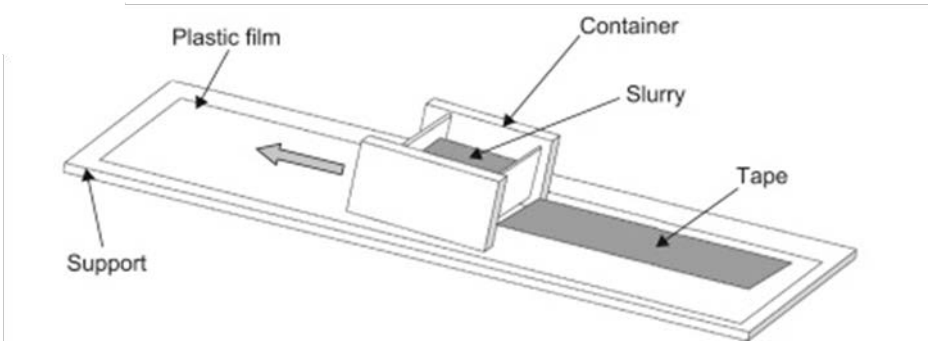

Figure 6. Manual tape casting apparatus used for cold ceramic tapes, often with electronic applications. **[18]**

For patterning, a method such as flexographic or screen printing may be utilized. This process requires additional handling and direct contact with a metal or plastic stencil. Care must be taken to prevent introducing contaminants in this step. Ink is applied and a squeegee is used to spread the ink over the mask, removing any additional ink. The stencil can be reused making it a relatively inexpensive process. This method has been utilized to achieve 2D solid state lithium-ion batteries with complex designs [15].

After the coating process the tape is heated, typically under vacuum, to remove any solvent. Residual solvent will decrease the conductivity of the battery. The final coating will shrink during the drying process depending on the viscosity and concentration of the slurry. Slurries with nano-sized particles are prone to forming micro

porosity in the tapes while slurries with large particles tend to shrink significantly. A compression step, such as calendaring is often used to reduce porosity in the tapes. Calendaring refers to a process where the material is passed through two rollers set at some desired thickness. As the rollers are rolled the material passes through the small gap and the thickness decreased to the gap size of the rollers. Electrodes with porosity between 30-40% have shown the best electrochemical performance. Some porosity is helpful to ensure the electrolyte will be in good contact with as much cathode as possible. Too much porosity can cause the active material to be segregated which means there is no path available for ions to travel and they will not contribute to the reaction [4].

The rheological properties and composition of the slurries have a huge impact on the performance of the battery. Slurries for this coating method must be highly viscous and homogenously dispersed. The slurry must be shear thinning, once the doctor blade has passed over the slurry it should not flow so it will maintain its thickness and position on the substrate. The viscosity and height of the doctor blade directly impacts the thickness of the final tape. As the tape dries the thickness will reduce by approximately 50% depending on the slurry composition. Inhomogeneity will result in inconsistencies within the tape including areas that have a lower concentration of active materials or poorly distributed carbon. The slurry should be stable for a few days especially in high production facilities where the slurry may sit for some time before coating can occur. Stability over this time period means the dispersion will not segregate through sedimentation, coagulation or Ostwald ripening (where small particles dissolve and deposit onto larger particles). At higher viscosities the kinetic energy of the particles is decreased which reduces the likelihood of sedimentation. In the cathode's high viscosity

slurry, the interactions between the binder, carbon, and active material create a “weakly coagulated state that allows an interconnected network of conductivity” [19, 20].

The slurry chemistry is vital to producing a tape of the desired thickness and composition but this limits the slurry compositions that can be used successfully. A large amount of powder and/or additives go into making the proper shear thinning viscous slurry. These properties are tailored by adjusting the ratio of the binder, carbon and active materials in the solvent. The method and order in which these components are mixed plays significantly impact the resulting tape. Dispersants and other additives may benefit the rheological properties but it is best to choose a solvent that does not require additives that will reduce the concentration of active materials.

II. Literature Review

Chapter Overview

The purpose of this chapter is to review relevant research on topics pertaining to the research conducted in this document. Specifically printing methods for battery materials. Printing methods have been heavily utilized in different technologies including circuits, solid oxide fuel cells (SOFCs), and solar panels. Automated printing systems allow for high precision placement of the inks resulting in unique geometries or patterns that cannot be achieved in methods like blade coating. As the technology advances we are able to achieve smaller and smaller features resulting in better performance, particularly for electronics. In many cases the system can be fully automated in attempts to eliminate human related errors. This allows for higher throughput and lower cost than many traditional methods.

Extrusion Based Printing

3D printing is used to print a broad range of materials and is a fast-growing process that has been used for numerous applications [15]. One type of 3D printing is extrusion or dispenser based printing, which uses a syringe to deposit ink over a substrate. The rate of printing is controlled by the pressure in the ink barrel. The opening of the needle ranges from 0.5-400 μm and a wide range of ink viscosities are viable for this method. The behavior of the ink and needle size determines what pressure must be utilized to achieve the desired printing rate. It is difficult to prepare ink for this method as the suspensions can have differing local ink densities due to large particle size distribution and the differing particle densities of the active material and additives. Smaller particles are

preferred to prevent the needle from clogging. To prevent sedimentation the fraction of solvent is kept to a minimum resulting in high viscosities that require higher pressures to print and may result in unwanted porosity. As the ink is placed if it is too viscous to flow further placing a second layer may result in porosity [4]. A shear thinning ink is desired and it has been shown graphene oxide produces desirable viscoelastic properties when prepared in an aqueous dispersion. With high concentrations of a gel like ink it can be used to print fine or complex architectures which may be utilized in tiny energy storage devices. These types of ink formulations have been used to print interdigitated batteries as shown in **Figure 3** [15].

Extrusion or dispersion based methods are slow for printing large areas when compared to other methods but excel at printing patterned areas such as 3D interdigitated batteries or extremely small batteries for microelectronics. This method has been utilized in various applications including the production of small thermoelectric generators, batteries, and ceramic structures [4, 13, 21].

3D interdigitated architectures were created for micro-batteries with lithium iron phosphate cathodes and lithium titanate anodes as seen in **Figure 3**. The inks were printed and annealed to form a connected porous structure. Results were obtained using a liquid electrolyte and were comparable to similar batteries. These architectures allow for high aspect structures that occupy a small areal footprint while maintaining small transport length scales for ion and electron transport. Further work is suggested to include printing a liquid or gelled electrolyte [21].

Wei et al. has utilized 3D printing to print a square cell battery. Every component of the battery was printed including the casing and all internal components. The electrodes were printed on a glassy carbon substrate, which acts as the current collector for these batteries. The printing method produced thick electrodes and allowed for the elimination of the drying and calendaring step, as well as, electrolyte infilling and heat-sealing processes associated with conventional methods. To achieve the desired viscosity biphasic inks were created using lithium iron phosphate and lithium titanate. The batteries achieved high areal capacity as compared to values from literature [13].

Spray or Aerosol Printing

Spray or aerosol jet printing is similar to airbrushing. Compressed gas is passed at high velocity over an open tube creating a pressure differential. The pressure in the container is high enough to atomize the ink as seen in **Figure 7** which is transported by a carrier gas through a nozzle towards a substrate. The particles must be stable with in the ink for the entirety of the printing time to ensure homogenous droplets are formed. The ink may be agitated to help mitigate settling during the printing process. If these conditions are met this process works for inks with a wide range of viscosities (1 to 1000 cP). Often high viscosity inks are harder to atomize so stability and fluidity must be balanced to achieve a printable ink. The ink can be heated during printing which can help lower the viscosity and may help the ink dry during the coating process when using low vapor pressure solvents [4].

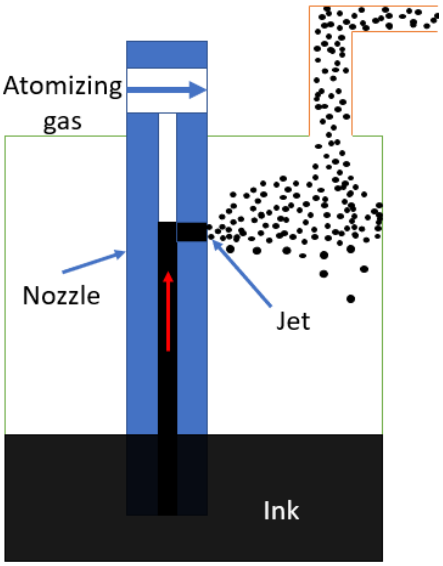

Figure 7. Schematic of a pneumatic atomizer.

Atomization can be achieved through a pneumatic or ultrasonic atomizer. Pneumatic atomization uses the Venturi effect described previously to suction ink through a nozzle. The ink is then shot at the wall of the ink jar to create droplets. The number of jets or openings for the ink to be expelled can be adjusted depending on the composition of the ink. Droplets between 1-5 μm are sent up through the print head while larger droplets fall back into the ink pool. This method works best with inks between 1-1000 cP. Ultrasonic atomization uses an ultrasonic transducer to create high frequency pressure waves that travel into the ink causing the ink to disperse into droplets. This method works best with inks between 1-5 cP and with particles less than 50 nm. The ultrasonic method works for a smaller range of inks but it produces less waste and can have higher throughput. Once the droplets are produced, by either method, an inert gas acts as a sheath gas directing the droplets as they exit the print head. The atomization and sheath pressures can be adjusted before printing.

The process can be effective on rough surfaces or complex geometries such as foams or meshes. The area that can be printed is only limited by space. Multiple layers may be printed to increase the thickness. Each pass will only build up microns of thickness so it is a relatively slow process and time can be another limiting factor. By modifying the size of the nozzle and the printing speed it is possible to create a set up that will result in higher volume production of larger areas than are capable with standard methods.

It is possible to print two inks that are blended as the ink reaches the printer head or one directly after the next which means all layers of the battery, cathode, electrolyte, and anode, can be printed onto the same substrate with little to no additional handling. This ensures good contact between the layers and introduces the ability to functionally grade two different inks. Spray printing has been used to deposit active layers for electrodes, solar cells, super capacitors and solid oxide fuel cells.

A group from Rice University used a manual spray-painting technique to create battery components including a $LiCoO_2$ cathode, polymer separator, and Lithium Titanium Oxide (LTO) anode. Each layer was sprayed directly on top of the preceding layer on a variety of substrates including glazed ceramic, glass, stainless steel, and flexible polymers. Batteries were produced within 10% of the theoretical capacity with an 89% success rate over multiple sprayed cells [22]. This method could be easily integrated into existing processes. If sprayed batteries could be placed on a roof with solar panels placed directly on top of them, the energy loss from the solar panels could be reduced significantly.

An aerosol jet printed thick, 170 μm, $LiFePO_4$ cathode was fabricated by Deiner et al with a specific capacity of 151 $mAhg^{-1}$ after a C/15 discharge rate. The ink consisted of LFP, Carbon Super P and Kynar 1800 in a 92:3:4 ratio by weight percent suspended in a mixture of 2-Butanol and N-methyl 2-pyrrolidone (NMP). The ink was aerosol jet printed onto a heated plate with a carbon coated aluminum substrate. The resulting tapes were dried and then tested in coin cells using lithium metal as the anode and a liquid electrolyte. These cathodes showed aligned needles on the surface and submicron pores throughout the cathode which is not found in typical casting methods, as seen in **Figure 8**. These features could be utilized to create cathodes with unique microstructures that would allow for better electrolyte penetration and interconnected pathways for ion movement [1].

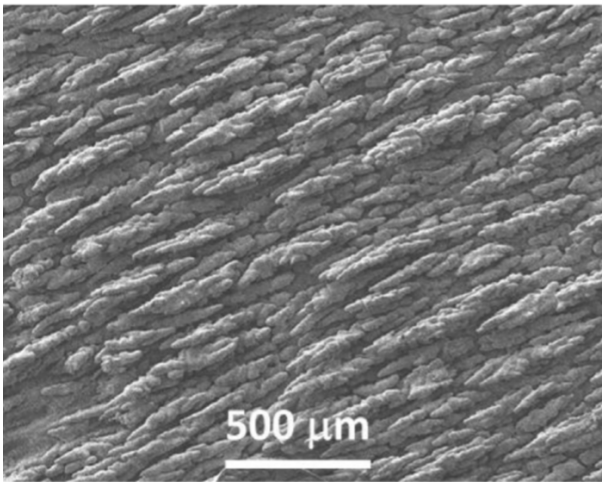

Figure 8. Top down secondary SEM image of aerosol jet printed $LiFePO_4$ cathode with 93.7% $LiFePO_4$, 1.8 wt% Super P Carbon, and 4.5 wt% Kynar 1800 binder **[1]**.

A group from the University of Oxford spray printed lithium titanate and lithium iron phosphate electrodes with varied conductive additives, thicknesses, and weight ratios of materials suspended in an aqueous solvent. Although the electrode surfaces were not flat,

the same needles were not seen in these printed cathodes demonstrated in Deiner's work. No calendaring was required on the printed electrodes to achieve results comparable to tape cast electrodes indicating the printed electrodes may have helped minimize the inaccessible areas within the electrode [23].

III. Experimental Procedure

Chapter Overview

The purpose of this chapter is to explain the techniques utilized to fabricate and characterize the cathode tapes and resulting batteries.

Ink Preparation and Design

Nine lithium cobalt oxide ($LiCoO_2$) inks were created for Optomec ultrasonic aerosol jet printing. The compositions were based on three different ratios of the solids by weight percent ($LiCoO_2$/Conductive Carbon/Binder) and three different percentages of total solids by volume for each ratio as shown in **Table 1**. The active material for the cathode slurries is $LiCoO_2$, Lithium Cobalt (III) Oxide (Sigma Aldrich, 99.8%). The conductive carbon powder is Timcal Graphite and Carbon Super P® conductive carbon black (MTI, Inc.). The binder used in the cathode ink is Kynar 1800 (Arkema), polyvinylidene difluoride (PVDF) with an industry tailored molecular weight to improve adhesion and conductivity. To achieve the appropriate viscosity and reasonable vapor pressure, particles were suspended in a solvent mixture consisting of a 1:3 ratio of 2-Butanol (Alfa Aesar, 99%) and N-methyl 2-Pyrrolidone (NMP, Sigma Aldrich, 99.4%) selected based on the Hansen solubility parameter for PVDF. The weight of solvent was kept constant for all nine inks, thereby allowing the change in powder ratios and volume percent solids to supply a range of viscosities to be printed.

Table 1. Printed Inks Solids Loadings in terms of Volume and Weight

	80/10/10			90/5/5			95/2.5/2.5		
Volume %	12.4	15.5	21	12.4	15.5	21	12.4	15.5	21
Weight %	13.1	16.3	22	17.9	22	29.1	22	26.8	34.6

Active Particle Manipulation

The ink design was based on the tape cast recipe provided on the MTI Corporation website and work done by Deiner on lithium iron phosphate ($LiFePO_4$) cathodes [1]. The larger and plate-like shape of the $LiCoO_2$, as shown in **Figure 9**, made it difficult to suspend when compared to the low viscosity inks used when making the $LiFePO_4$ cathode tapes. To address this, additional steps were performed while mixing the ink to help break down the particle size of the $LiCoO_2$ material.

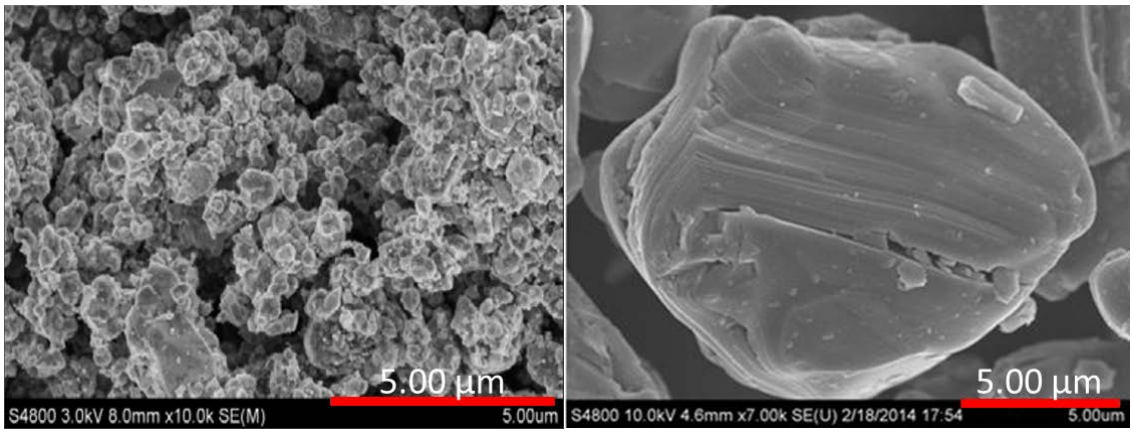

Figure 9. *Left)* As received $LiFePO_4$ particles. Particle size is between 1-2 microns. Image courtesy of MTI Corporation. *Right)* As-received $LiCoO_2$ particles. Particle size is between 5 and 15 microns. Image courtesy of Sigma Aldrich.

The $LiFePO_4$ particles shown in the above figure are more spherical and smaller than 3 μm making suspension relatively simple in Deiner's previous work. The $LiCoO_2$ powder, as received from Sigma Aldrich, has particle sizes between 5 and 25 μm. Particles of this size tend to clog the printer jets. In addition, the crystal structure of the material leads to platelet shaped particles which are difficult to suspend in the low viscosity solution required for printing. Few commercially available powders have smaller particle size than the Sigma Aldrich powders. The processing involved in synthesizing smaller particles is time consuming making it very expensive. Many of these synthesis methods can block the lithium ion pathways which could have a negative effect on the batteries. Different methods were attempted to create a more accommodating particle size and shape including; vacuum mixing(a process is used in tape casting), shaker milling, synthesizing nano-particle belts, and a multi-step ball milling process that most closely resembled Deiner's process. All methods were preceded by hand mixing the carbon and $LiCoO_2$ using a mortar and pestle to encourage the coating of the $LiCoO_2$ particles by the carbon.

A large amount of settling occurred after vacuum mixing. The particles were not transformed in any way and remained difficult to suspend for low viscosity printer inks. The shaker milling, synthesized nano-particles and ball milling methods proved relatively successful at reducing the size of particles and tapes were printed for each of these. The powders and printed tapes can be seen in **Figure 10**.

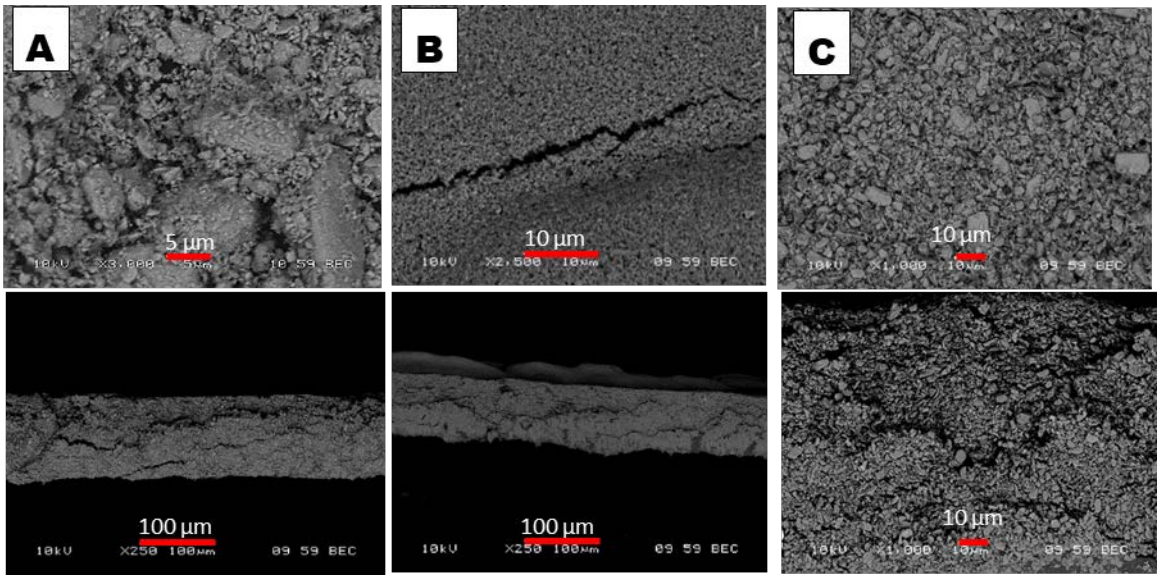

Figure 10. The top row shows the particles before printing, the bottom row shows the resulting tape of the particles directly above. A) Particles shaker milled for 4 hours, produced a wide distribution of particle sizes resulting in highly packed dense cathodes. B) Synthesized nano-particles, agglomerations present. Formed great inks but need to be studied more thoroughly to tailor their electrochemical properties. C) Particles roller milled for 192 hours with graphite.

The shaker mill created extremely small particles with some rounding but after 4 hours the size distribution became rather large. This led to a densely packed cathode causing reduced flexibility and a brittle tape that proved hard to handle. The tape delaminated, or became disconnected, from the current collector and flaked at the edges when a shape was cut out for the battery formation. Additional sieving steps could be utilized to minimize the particle size distribution but sieves can still allow long thin particles to pass which would be present in the final ink.

The $LiCoO_2$ synthesis proved successful at making a variety of particle shapes. The only shape that could be produced in bulk (10's of grams per synthesis) were belt shaped which had one long axis and a shorter nano-sized width. A short mixing process was utilized but the ball milling still broke the belt shapes into smaller nano-sized semi

spherical particles. The nano-particles were stable in suspension and produced a dense tape. Neither the tape cast nor the printed tape utilizing the synthesized powders proved successful under electrochemical testing indicating there may be issues with the powder itself. Further investigation into the synthesis process will be necessary before this material will be ready for batteries but once this synthesis process is perfected aerosol jet printing may be a beneficial technique to fabricating these cathodes.

A ball milling process with all of the components of the battery, such as Deiner used [1], was compared to a two-step process. The two step process was broken into a higher viscosity mixing step to decrease particle size and a short mixing step to incorporate the binder and remaining solvent. Both inks were mixed for over 200 hours monitoring particle size reduction at 24 hour increments. The two-step process appeared to reduce particle size more quickly and the performance of the batteries made from this tape were comparable to the one-step process. It is believed utilizing the two step process may allow reduction of mixing time depending on the ink composition.

The two-step ball milling process consisted of 203 +/- 13 hours of roller milling with the $LiCoO_2$, carbon, and a reduced amount of NMP followed by an additional 24 +/- 2 hours of roller milling with the binder and remaining solvent. The ball milling occurred in a glass jar with cylindrical yttria-stabilized zirconia milling media, 5mm diameter by 5 mm height. Cylindrical media was used over spherical media to help reduce the particle size by increasing the surface area participating in applying the force. Spherical media would be preferable if only mixing was required [24]. The addition of the carbon in the

first step increases the viscosity due to the high surface area of the carbon acting to stabilize for the $LiCoO_2$ and suspending the particles in the NMP throughout the mixing process, resulting in particle size reduction. This method was utilized for all testing in this paper unless otherwise mentioned.

Ink Viscosity

Flat plate viscosity measurements were taken with a LVDV-II+Pro Brookfield viscometer with a CPE-40 plate, shown in **Figure 11**. This viscometer and plate were chosen to accommodate the low viscosity ink. An added benefit is that this viscometer only uses 1 mL of ink the ink recipe did not need to be changed to create a large amount of excess material for viscosity measurement. The viscosity for each ink was measured before and after printing at 6 RPMs. The thickening of some of the inks after printing made it difficult to measure the viscosity at this speed and no result is reported for these inks. The viscosity is expected to increase slightly due to the evaporation and loss of solvent during the printing process, particularly the 2-Butanol due to its lower vapor pressure, 1.67 kPa at 20°C, as compared to NMP, 0.046 kPa at 20°. However, if there is an extremely large change in the before and after ink viscosities it may indicate the ink is less stable and settling occurred causing the solvent to print preferentially. Preferential printing of the solvent would leave behind more solids in the ink which would cause an increase in the viscosity in the ink container. If separation or settling occurs in these inks during the viscosity test the results for this test would not be valid.

Figure 11. LVDV-II+Pro Brookfield viscometer with a CPE40 plate.

Tape Cast Slurry versus Printer Ink

The primary difference between a tape cast slurry and an aerosol jet ink is the viscosity requirements. A tape cast slurry should be shear thinning and highly viscous. A high viscosity ink has high cohesion to itself and therefore will be difficult to aerosolize. A tape cast was created of the 95/2.5/2.5 solids ratio and with 54.5 volume percent solids loading and 80/10/10 solids ratio with 28.3 volume percent solids loading is also observed from an earlier study. This slurry was formulated with a more standard ink design, utilizing only NMP and shear mixing which does not result in any particle size reduction. This allow comparison between the electrochemical behavior of the as received particles and the particles that have been manipulated for printing. Any particle manipulation creates an opportunity for contamination or reduction of the electrochemical properties of the active materials.

For the tape cast slurry the binder was heated however this step was avoided for the printed inks. For the tape cast the NMP is heated to ~90°C to fully dissolve the binder however this increases the viscosity drastically, increasing the cohesion within the slurry. For the printed ink the binder is only partially dissolved overnight into room temperature solvent before being added to the other ingredients. Swelling occurs in the binder but it never fully dissolves at room temperature [17]. When the binder is heated and dissolved the viscosity increases greatly. The higher viscosity ink is more difficult to atomize and requires an increase in the atomizing pressure. This increase causes dripping from the print head and printing must be halted to clean the flooded system.

The 95/2.5/2.5 tape cast was performed with a doctor blade set to have a 200 μm gap. It was left in a dry room overnight before being transferred to a vacuum oven at 90°C overnight. The final thickness of this tape is 109 μm and the thickness of the 80/10/10 tape cast is 59 μm.

Printing Cathode Inks

An Optomec ultrasonic aerosol jet 200 printer with a custom steel print head and pneumatic atomization, shown in **Figure 12**, performed all printing in this study. All printing was performed in a temperature and humidity controlled dry room. The printing conditions for the Optomec printer were kept constant for all the prints. The atomizing pressure was set to 1500 cc/min and sheath pressure was set to 1000 cc/min, the nozzle had 2-jets. The pressure of the atomizer is monitored throughout the printing. Large changes in this value can indicate a clogged jet or issues with the ink during printing. 99.9% pure Nitrogen gas was used for the atomizer and sheath gas. A 1 cm x 1 mm

printer head opening was utilized. The printer head was set to 9 mm above the current collector substrate. The current collector (MTI carbon coated aluminum foil, 0.016 μm thick) was vacuum held to a plate heated to 45°C to aid in the drying. Ideal drying occurs when the tape appears dry, and loses its wet shine, before the next layer is placed. A 60 x 60 mm^2 area was printed moving the printer head in 2.5 mm steps between each sweep at a set speed of 100 mm/s. The print head has a 10 mm slot for ink deposition so each sweep had significant overlap. Each full layer took 2 minutes and 45 seconds to complete and a total of 50 layers were printed with each ink. The ink was kept at room temperature and a magnetic stir bar mixed the ink for the entire printing process to mitigate settling. The printed tapes were immediately transferred to an oven and dried at 90°C overnight to remove any solvents.

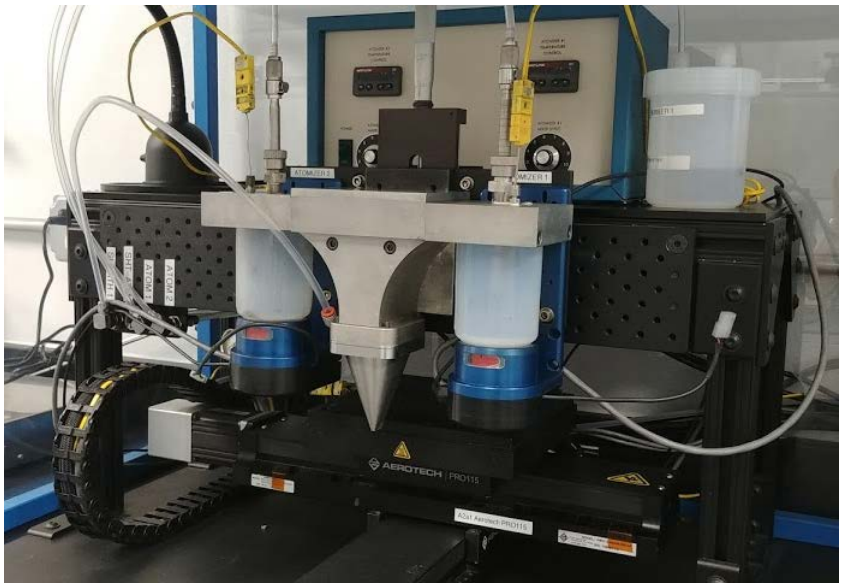

Figure 12. Optomec Ultrasonic Aerosol Jet 200 Printer and pneumatic atomizer.

Ratio of Solvent and Solids Printed

To measure the amount of material printed the printer head was held stationery and ink was sprayed into an aluminum weight boat for 5 minutes. The resulting weight was recorded and the weigh boat was dried with the printed tape. This post drying weight was recorded to determine the total weight of the active material, carbon and binder printed compared to the amount of solid printed. The difference between the wet and dry weights determined the amount of solvent printed. Four deposition rates were taken before printing and after 10, 20, 35, and 50 passes for a minimum of 8 deposition rates per print. Additional measurements were taken if there was a concern with the printing process, particularly if the atomizing pressure changes or there is a significant weight change between deposition rates. During the initial 4 rates the inside of the equipment is coated and the deposition rate increases slightly after each measurement is taken. After 15-20 minutes of printing this rate is relatively stable.

As the print progresses the solvent ratio will change due to evaporation within the ink container. If the ink is stable this change should not be drastic and the deposition rate will stabilize. The change will be drastic if there is instability in the ink that causes settling or particles that clog the nozzle. All of these events are reflected by either the change in atomizer pressure as mentioned above or a change in the deposition rate.

Each weigh boat was dried out along with the printed tape. The weight post drying was measured which allows the total weight of the solids after the solvent has been removed, to be calculated for each 5-minute period. This should relate directly to the amount of solids in the final tape. A further method described below allows the weight of the active material to be calculated after burning off the carbon and binder.

Tape Characterization

After printing the tapes, physical characteristics were measured utilizing flat-flat calipers to determine thickness of the printed tape. Secondary electron microscopy (SEM) was utilized to visually compare the tapes and any resulting microstructural features.

Thickness and Surface Morphology

The thickness of each tape was measured with flat-flat calipers and imaged with scanning electron microscopy (SEM, Jeol, JSM-6060). The bulk density of each tape was measured by taking the thickness and weight of a 5/8” disc of the cathode material. Backscatter SEM (BCE) was utilized to inspect the particle size and shape as well as the distribution of the carbon, binder, and any visible porosity. The surface morphology and cross section were examined utilizing secondary electron imaging (SEI). These measurements were used to relate the electrochemical results to the unique surface morphology achieved with the aerosol jet printing method.

Electrochemical Testing

Thermogravimetric analysis (TGA) measurements were made to determine the amount of active material printed as compared to what was expected based on the ink composition. This value is important when calculating the capacity of the battery for cyclic testing. Coin cell batteries were assembled and electrochemical testing was performed on the batteries including, constant charge and discharge cycling, cyclic voltammetry, and electrochemical impedance spectroscopy (EIS).

Weight Loss Study

To determine the ratio of $LiCoO_2$ in the final print, thermogravimetric analysis (TGA) was utilized on the dried samples obtained from the deposition rates. This allowed the weight loss to be monitored as the binder and carbon oxidize from the cathode material leaving the $LiCoO_2$ behind. The goal of this technique is to fully decompose the binder and carbon and measure the residual weight of the $LiCoO_2$ to determine the ratio of what was printed compared to the ratios of solid materials added to the ink.

A 50:50 ratio of Super P conductive carbon and Kynar 1800 binder was tested first to ensure they would decompose fully within the temperature limits of the TGA. The result is shown in **Figure 13**. Decomposition occurred by 600°C for the binder and 700°C for the carbon. There is some overlap between the decomposition regions of the two additives so it is not possible to determine the ratio of binder and carbon printed only the total weight of both. There was a very small residual weight left of these materials which does add to the error of this process.

A sample of $LiCoO_2$ powder was tested to ensure no reactions occurred within the relevant temperature range. No weight change was observed in the as received powder. As the particle size decreases this will not always be the case as is discussed later. Finally, a sample was taken from the tape cast material and tested to ensure this method could accurately measure the residual weight of a known amount of $LiCoO_2$ in a cathode also depicted in **Figure 13**. The residual weight was measured to be 79.52% in a tape cast material with 80% $LiCoO_2$ in the slurry.

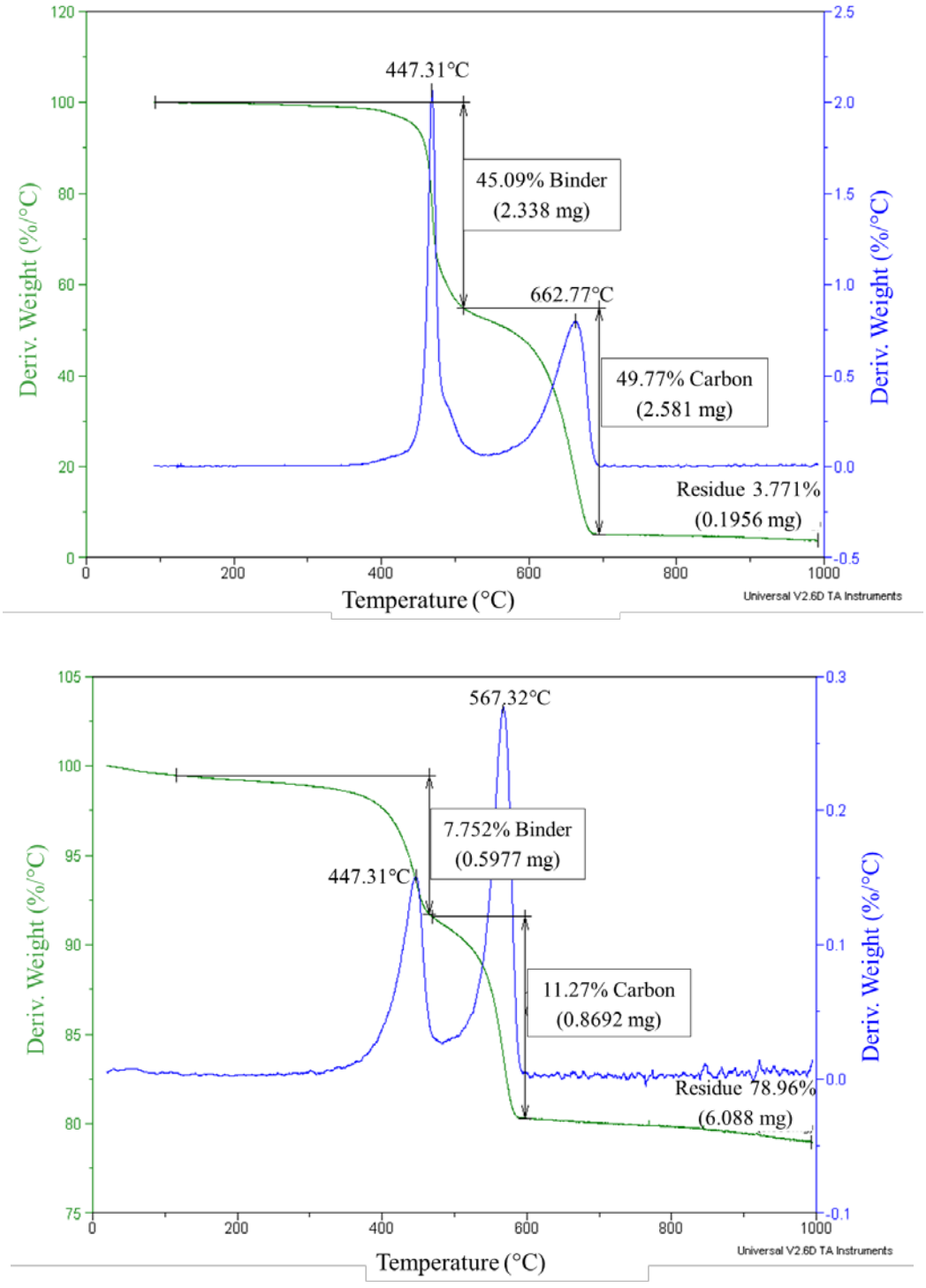

Figure 13. TGA tests were performed to ensure validity of results. *Top*) TGA results of a 50/50 mix of Super P Carbon and Kynar 1800 binder to determine approximate decomposition temperatures. *Bottom*) TGA of an 80/10/10 tape cast material to ensure correct amount of $LiCoO_2$ is measured (80%).

To measure the amount of active material present in the print, a sample was scraped from each weigh boat and placed in an alumina crucible. An attempt was made to test all material from the deposition rate at one time. Sample sizes ranged from 1.5 to 15 mg. The temperature was ramped at 5°C/min up to 1000°C. The $LiCoO_2$ residual weight was taken immediately after the second weight loss, between 500 and 750°C. This residual weight was recorded to determine the ratio of $LiCoO_2$ to non-active solids in the printed material. This process was used to determine what percentage of the active material was in the final print and to verify the printer was not preferentially printing the inactive materials. A $LiCoO_2$ decomposition was observed at higher temperatures, above 800°C, as described in equation 8 [25]. This was not observed in the as received powder due to the larger particle size. As the particle size decreased there was a more dramatic weight change attributed to the exposed surface area of the particles. Smaller particles tend to be more reactive due to the amount of surface area exposed.

$$\boldsymbol{Li_xCoO_2 \rightarrow xLiCoO_2 + \left(\frac{1-x}{3}\right)Co_3O_4 + \left(\frac{1-x}{3}\right)O_2} \quad (8)$$

Battery Fabrication

2032 sized coin cell batteries were fabricated to perform electrochemical testing. The printed cathode tapes were cut using a steel 5/8” punch into 5/8” discs and weighed to determine the bulk density and active material weights. The cells were assembled with a separator membrane (GE Healthcare, Whatman Glass Microfiber Filter), liquid electrolyte (LiPF6, Sigma-Aldrich, Battery Grade with 1% Vanadium Carbide added), and a lithium foil anode (149 microns, 5/8” diameter). Three batteries were made from each tape.

Cyclic Testing

A Landt CT2001A was utilized to test the charge/discharge capability of the batteries. Constant current charge and discharge cycles were performed on two batteries from each tape. The batteries were cycled for a total of 50 cycles at various C rates as shown in **Table 2**.

Table 2. Cyclic charge/discharge rates.

Number of Cycles	Charge	Discharge
1	C/20	C/15
4	C/20	C/10
5	C/5	C/5
5	C/5	C/2
5	C/5	C/5
5	C/5	C
25	C/5	C/5

The maximum capacity, C, was calculated using the weight of the active material based on the ratio of material in the ink as shown in equation 9. Based on literature values the usable theoretical capacity of the $LiCoO_2$ cathode is 140 $mAhg^{-1}$ and cells are cycled over the voltage range, 3.0V – 4.2V. To find the maximum capacity of the cathode in mAh the weight of the active material in a 5/8” disc was calculated using the ratio of active material and the weight of the cathode as shown in equation 9. To find the true capacity of the printed cathodes the capacity was recalculated based on the ratio found in the weight loss study to achieve a more accurate value.

$$Maximum\ Capacity, C = g * r * Q \quad (9)$$
$$g = weight\ of\ the\ cathode$$
$$r = Ratio\ of\ active\ material$$
$$Q = available\ capacity\ \left(140\frac{mAh}{g} for\ LiCoO_2\right)$$

The charge/discharge rates were selected based on established practice within the AFRL laboratories. By increasing the rate the batteries are placed in more strenuous conditions. The amount of decrease in performance as the rate is increased is monitored to determine the power density of the battery. As the rate is increased the ions will have less time to move from one electrode to the other, which leads to a lower capacity. If the batteries have a higher power density they will be less effected by the rate change. This is typically offset by a lower energy density. A larger cathode mass will typically take longer to reach 50% delithiation because it will take longer for the lithium ions to diffusion through the battery.

A decrease in capacity is also expected over time due to a resistive layer that slowly forms due to inefficiencies in the reaction that allow unwanted products to form. Typically batteries last more than 200 cycles so there should be very little time related capacity decrease over the 50 cycles tested.

Electrochemical Impedance and Cyclic Voltammetry

Cyclic voltammetry and EIS measurements were performed on a single battery from each tape using a Solartron Potentiostat/Galvanostat. Four impedance measurements were made and a cyclic voltammetry cycle was performed between each impedance sweep.

For electrochemical impedance spectroscopy, an AC voltage of 10 mV was applied for frequencies ranging from 1 Hz to 1MHz when the battery is at its lowest charge. The real resistance (Z') and imaginary complex (Z'') response is recorded and graphed to create a Nyquist plot to find the various resistances in the battery. When Z'' equals 0 the real Z' response is equal to the ohmic resistance of the electrolyte. As the frequency increases there is a dip in the Z'' value and this dip can be extrapolated to find the charge transfer resistance. The ohmic resistance was measured to determine the performance of the cell as a whole and the charge transfer resistance is recorded to determine the ability of the lithium ions to migrate between the electrodes. These results are compared to a tape cast sample to determine if the printing process effected the cathode resistance.

The first two cycles were performed to condition the battery and the final cycle is reported in the results and analysis section. For cyclic voltammetry, the cell was cycled with a C/10 charge/discharge rate from 3.4 to 4.2 V. An example of the expected results can be seen in **Figure 1**

IV. Analysis and Results

Chapter Overview

The following section discusses what was expected to occur based on the varied ink compositions, the results achieved from the procedures described above, and finally analyzes how these results compared to the expected results.

Ink Rheology

The solvent was the same in each ink so the viscosity of the ink would be expected to increase with increasing binder content. Although the 95/2.5/2.5 inks have a higher solids loading by weight, the binder has a greater effect on viscosity as a stabilizing polymer and the high surface area of the carbon leads to increases in the viscosity. Thus, the 80/10/10 would be expected to have the highest viscosity. Based on this it can be beneficial to look at the weight percentage of binder in solvent, which for these inks is equivalent to the weight percentage of carbon.

It is expected, with higher percentages of solids there would be an increase in viscosity. The 21 volume percent ink is expected to be more viscous than the 12.4 volume percent when examining the same ink composition. With an increase in viscosity there will be an increase in the cohesion of the ink. Higher viscosity ink would be expected to be more difficult to atomize when holding the atomizing pressure constant. As a result, the microstructure formed may appear different than an ink with lower cohesion.

The amount of solids and binder in the ink as well as the viscosity of the ink before printing, measured with the Brookfield Viscometer is shown in **Table 3**. Each value is taken from one sample or the average of two samples, as some of the samples were not measurable due to concerns with the viscometer. **Figure 14** shows the percent of binder as compared to the measured viscosity. It is clear from these measurements we did not see the expected results or trends. The 21 volume percent inks had the highest viscosity in all cases but the 15.5 volume percent inks had the lowest viscosity measurement when compared to the other inks with the same solids ratio. This may be an indication that choosing one mixing method for all ink compositions, while ensuring consistency, does not provide the most stable ink for each composition. Tailoring an ink can be a difficult and time-consuming process but is important to ensure the quality of the finished product. As will be shown throughout these results, the low viscosity measured for the 15.5 volume percent inks did not appear to effect the quality of the tape, except in the case of the 95/5/5 ratio. Therefore these viscosity results are believed to be unreliable.

Table 3. Weight percentages that factor into the viscosity measurements taken of the ink before printing.

	Total Solids in the Ink	% Binder in Solvent	Viscosity Before
	wt %	wt %	cP
80/10/10, 12.4 vol%	13.1	1.51	16.4
80/10/10, 15.5 vol%	16.3	1.95	6.7
80/10/10, 21 vol%	22.0	2.83	43.8
90/5/5, 12.4 vol%	17.9	1.09	21.1
90/5/5, 15.5 vol%	22.0	1.41	17.4
90/5/5, 21 vol%	29.1	2.05	33
95/2.5/2.5, 12.4 vol%	22.0	0.71	18
95/2.5/2.5, 15.5 vol%	26.8	0.91	16.9
95/2.5/2.5, 21 vol%	34.6	1.32	33.1

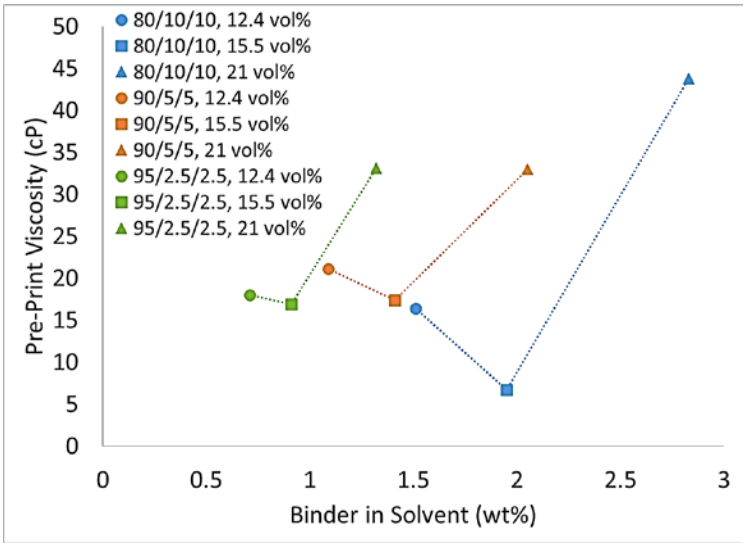

Figure 14. The weight percentage of the binder in the solvent versus the before printing ink viscosity. The viscosity was expected to follow a linear trend, increasing with the increasing amount of binder in the solvent. This is not the case and the measurements are believed to be unreliable.

To achieve accurate viscosity measurements the suspension of particles must be uniform within the ink. At low viscosities this is difficult to achieve and the active materials within less stable inks will settle. If these inks are not stable it would be possible to achieve inaccurate viscosity measurements using this technique. Larger quantities of ink would be required to achieve a full rheological profile and the resources were not available for this study.

The binder was not heated for the printed ink, and is not fully dissolving into the solvent. This allows the viscosity of the ink to remain in a range that is more easily printed however, as the weight percent of binder increases it is assumed there is less dissolved binder or less swelling of the binder because there is proportionally less solvent. This may be a factor contributing to some variance in the viscosity results. If the binder is not fully dissolving the carbon could be playing a larger part in these inks when it is a significant portion of the total ink composition.

There are many factors that could lead to an inaccurate viscosity measurement. A more in-depth viscosity profile may better define the rheology of the ink. Most methods require a significantly larger amount of ink than was produced for this study. Cohesion of the ink could also be studied by measuring the wetting angle however this was not available at the time of this study.

Ratio of Solvent and Solids Printed

The weight of the ink sprayed into a weigh boat for 5 minutes was compared to the weight of that same boat after it went through an overnight drying process. The weight lost is the amount of solvent printed and the weight remaining is the weight of the

solids including, the carbon, binder and $LiCoO_2$. The percentage of solids in these samples are compared to the percentage of solids in the ink by weight. An ideal print would see no difference between these values indicating the aerosolized droplets contained the expected amount of solids as compared to the amount of solvent. If there are fewer solids, the solvent is printing preferentially leaving more of the solids in the ink container once the print is finished. Losing the solvent from the ink container will shorten the life of the ink and the ink viscosity remaining in the container would be expected to increase dramatically making it difficult to atomize the ink the longer you print. This is indicative of an unstable ink. Backscatter SEM was utilized to see the particle size and shape after printing.

The values for the last 5 deposition rates were used to find the average weight percentage of solids printed which most accurately represents the solids in the printed cathode tape. The first 3 measurements were taken as the ink was coating the inside of the printer and the deposition rates are lower than the 5 taken during the printing process. These 5 values are believed to be most representative of the actual printed tape. The average solids weight are shown in **Table 4**. In every case the weight percent of solids in the printed tape is lower than the weight percent of solids in the ink. This can be correlated to the increase in viscosity in each ink after printing. Small changes are expected based on the aerosolization process however large changes may indicate instability in the ink. The difference in the expected solids versus the measured solids and the before and after ink viscosities is graphed in **Figure 15**.

Table 4. Measurement of the actual solids printed and the before and after viscosities. An increase in the viscosity indicates a loss in solvents proportional to the amount of solids being printed. This indicates instability in the ink.

	Total Solids in ink	Measured Solids Printed	Viscosity	
			Before Print	After Print
	wt %	wt %	cP	cP
80/10/10, 12.4 vol%	13.1	3.1 ± 0.7	16.4	29.8
80/10/10, 15.5 vol%	16.3	16.0 ±1.0	6.7	8
80/10/10, 21 vol%	22.0	16.6 ± 0.9	43.8	-
90/5/5, 12.4 vol%	17.9	17.2 ± 0.5	21.1	46.4
90/5/5, 15.5 vol%	22.0	21.6 ± 0.8	17.4	22.1
90/5/5, 21 vol%	29.1	23.3 ± 1.4	33	-
95/2.5/2.5, 12.4 vol%	22.0	19.8 ± 0.5	18	24.6
95/2.5/2.5, 15.5 vol%	26.8	4.0 ± 1.4	16.9	25.5
95/2.5/2.5, 21 vol%	34.6	23.9 ± 0.5	33.1	37.7

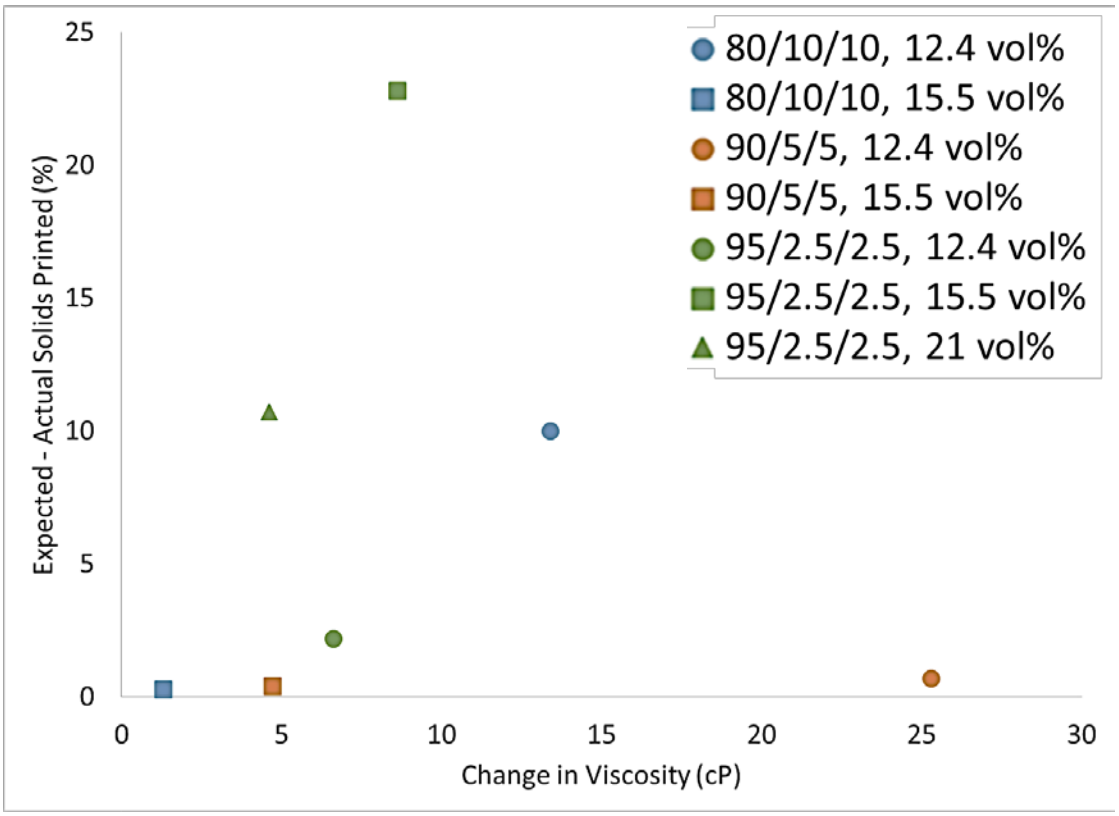

Figure 15. The change in viscosity is compared to the decrease in the solids printed when compared to the percentage of solids in the ink. A large change in the viscosity is expected to correlate to a large change in the expected solids printed. In most cases this is true and variability may be attributed to poor viscosity measurements.

When fewer solids are printed it does seem to relate a larger increase in viscosity except in the case of the 90/5/5, 12.4 volume percent and the 95/2.5/2.5, 15.5 volume percent ink. The first ink has the largest viscosity increase while maintaining a relatively small decrease in the ratio of solids printed. The second had a large change in expected solids while maintaining a lower change in viscosity. While there seems to be some correlation in all cases the ratio change within the ink does not seem to be the only factor in the viscosity change.

Two inks exhibited a large change in the expected solids printed which is accompanied by a large increase in the viscosity. To investigate the two inks that printed a low solids content the values obtained for each deposition rate, the 4 before printing started and the 4 taken at intervals during printing, were graphed in **Figure 16** to show the progression of solids printed for each cathode tape. There was little change over time for the majority of the prints. For the two prints that exhibited a low solids content (80/10/10, 12.4 volume percent and 95/2.5/2.5, 15.5 volume percent) this chart shows both prints start with >14 wt% solids printing and at some point before the printing begins this drops off to the average 3-4% as shown in **Table 4.** The weights taken during printing did not exhibit such a large change indicating more solvent is printing than is anticipated. At some point the ratio of solvent to solids changed. Both tapes were printed within one week of each other and it was noted during the printing the tapes appeared wet as if they were not drying properly.

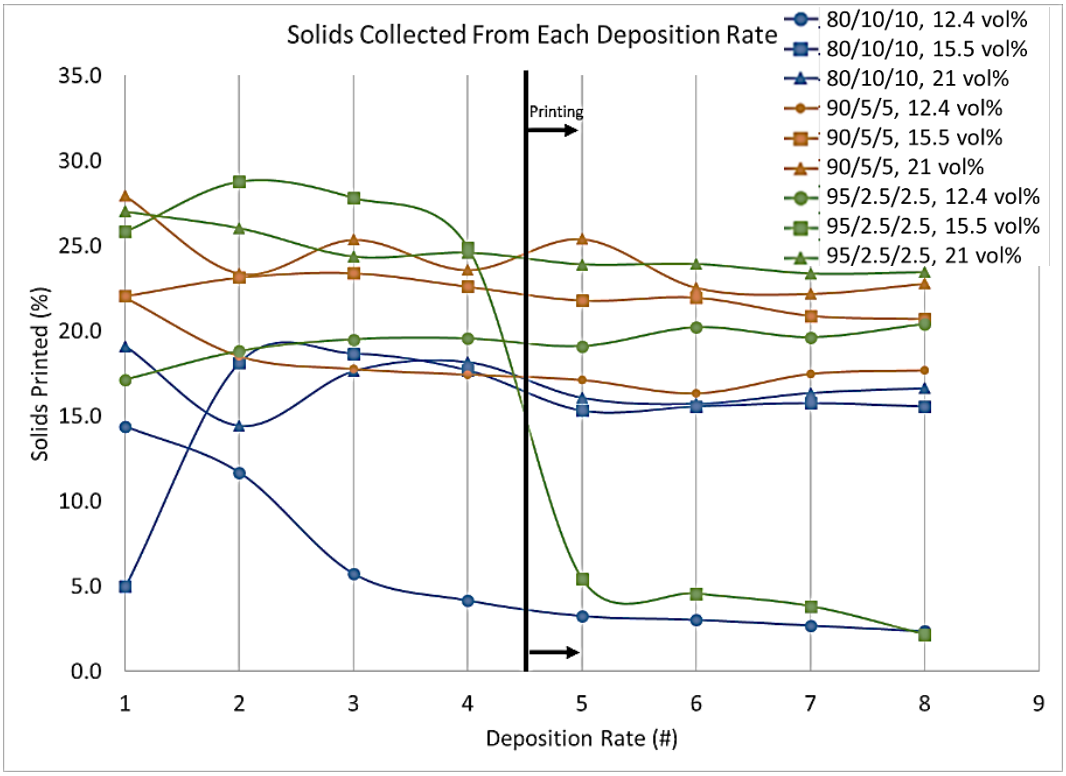

Figure 16. The percent of solids in solvent was collected from each deposition rate. Four collections were made before printing began and four collections were made in between print passes. The average value from the last four collections was used to determine the approximate amount of solids in the printed cathode.

Backscatter SEM images were taken of the printed tapes as seen in **Figure 17**. The Z contrast between the heavy $LiCoO_2$ particles and the carbon and binder make it easy to see the particle size and distribution using this method. The heavier $LiCoO_2$ particles show up as white and the carbon containing additives are black. The printed tapes have particles under 10 μm due to the ball milling. The change in size is evident when comparing these to the tape cast print, as seen in **Figure 18**. These particles appear unchanged from the as received material shown in **Figure 9**.

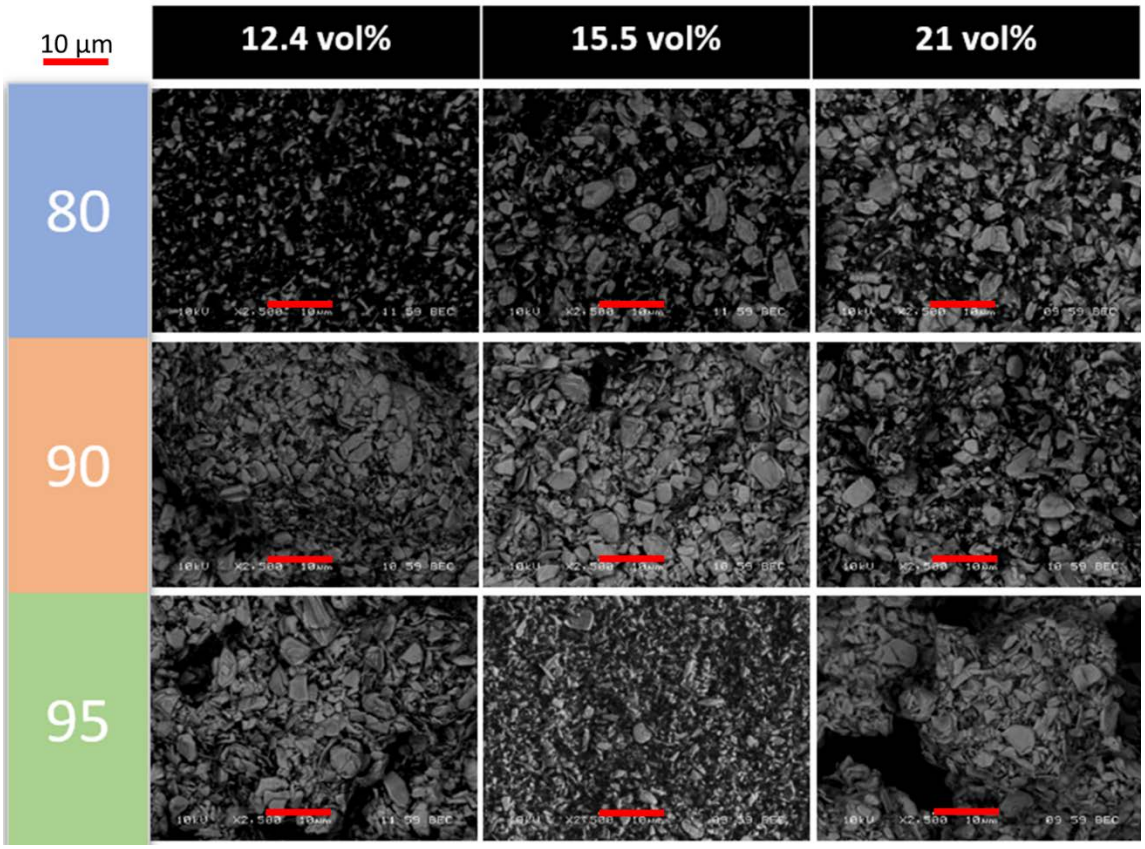

Figure 17. BEC-SEM images taken at 2500x, depicting the 9 cathode tapes and size of the particles after printing. The white particles are $LiCoO_2$ and the black regions are either, binder, carbon, or porosity.

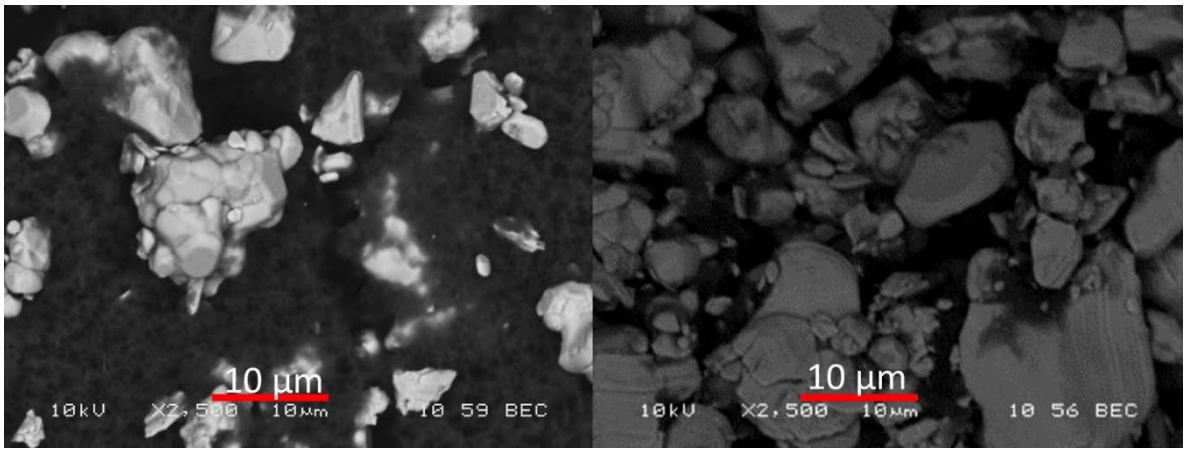

Figure 18. BEC-SEM image of the *Left)* 80/10/10 and *Right)* 95/2.5/25 cathode tape fabricated with the standard tape casting process, depicting the particle size. The white particles are $LiCoO_2$ and the black regions are either, binder, carbon, or porosity.

As will be seen later the $LiCoO_2$ cathodes had surface features similar to those seen in Deiner's work [20] and while it is difficult to see at this scale, this is evident in the porosity within the backscatter images. Like the $LiFePO_4$ tapes, these features are made up of densely packed regions of active material with carbon and binder distributed throughout. As would be expected the 80/10/10 tapes have a larger distribution of carbon and binder and there is very little visible in the 95/2.5/2.5 tapes in comparison. The porosity created as a result of these features will be discussed later.

Another item of note, both of the tapes with the lowest solids printed (80/10/10, 12.4 volume percent and 95/2.5/2.5, 15.5 volume percent) appear to have the smallest particle size in the printed tapes. This suggests the large particles were unable to aerosolize indicating there may be an issue with the ink or with the print nozzle. During printing the atomizing pressure is monitored. A large change in this pressure will indicate a change in the printing conditions such as a clogged nozzle. No change was noted during either print. It would appear that something occurred during these prints that caused both of these tapes to act as outliers. As the cause is unknown, the data is still presented within this paper. These results reinforce the difficulty of this method and shows that there are still many unknown factors that will affect the quality of printed cathodes.

Tape Characterization

More solvent in the printed tape may result in higher porosity once the solvent is removed. The amount of solids printed, specifically the amount of $LiCoO_2$ should directly impact the thickness of the printed cathodes, but if the porosity is changing or features are building this may not be the case. This would then be reflected by the bulk density measurements of the printed tape. A thick and dense cathode will have more material and thus the highest calculated maximum capacity in mAh. If the material is inaccessible then the full capacity will not be reached during the discharge cycle. If the material is too porous and there is no conductive path then the measured capacity will be lower than what is calculated.

Thickness measurements were taken with a flat-flat micrometer which captures any surface roughness as seen in the SEM images in **Figure 19**, **Figure 20**, and **Figure 21**. The print bulk density was calculated using the weight of a 5/8" disc cut from the cathode tape and the thickness measurements. The thickness and densities are shown in **Table 5**. Each tape consists of 50 passes.

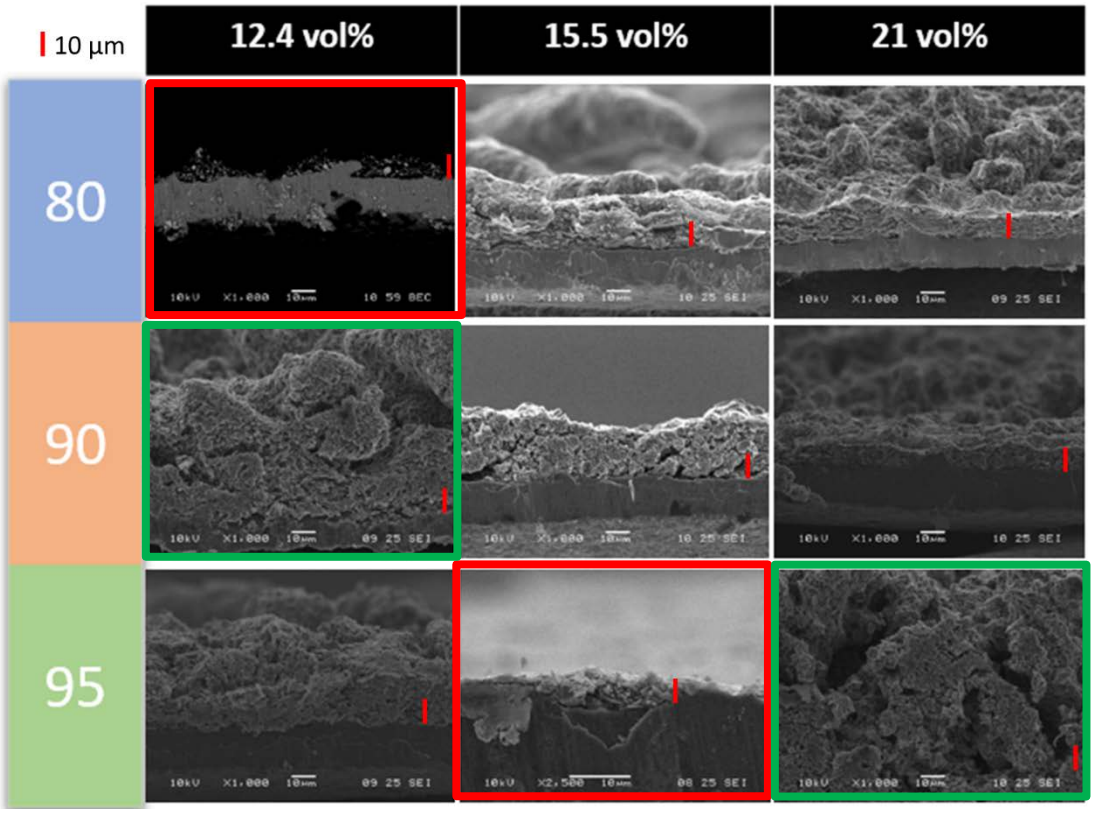

Figure 19. Cross-sectional SEM images of the 9 cathode tapes showing porosity and thickness. Images were taken at 1000x and the 10 µm bar is highlighted in red. The interconnected porosity compared to the denser cathodes is of interest when producing a battery with high specific capacity. The tapes outlined in green produced the most interconnected porosity while the tapes outlined in red are considered outliers.

The printed tapes each have a different size and shape to the surface morphology that results in a different porosity throughout the tape. The 90/5/5, 12.4 volume percent and 95/2.5/2.5, 21 volume percent both exhibit interconnected porosity that makes its way throughout the tape. It is easy to picture the electrolyte infiltrating into this cathode which will result in better ionic transfer. The 90/5/5, 12.4 volume percent tape has porosity along the current collector which may lead to delamination issues. For the 90/5/5, 12.4 volume percent tape there is no porosity coming from the surface and while this may be less dense than the tape cast the electrolyte will have trouble accessing these

areas. The rest of the tapes appear to be fairly dense with a rougher surface layer. The outliers are dense with no surface features. The denser tapes may sacrifice energy density for power density. Too much porosity can lead to delamination at the current collector. The channels and pores created by printing appear to reach down to the current collector however these tapes were able to maintain flexibility with no visible delamination or flaking.

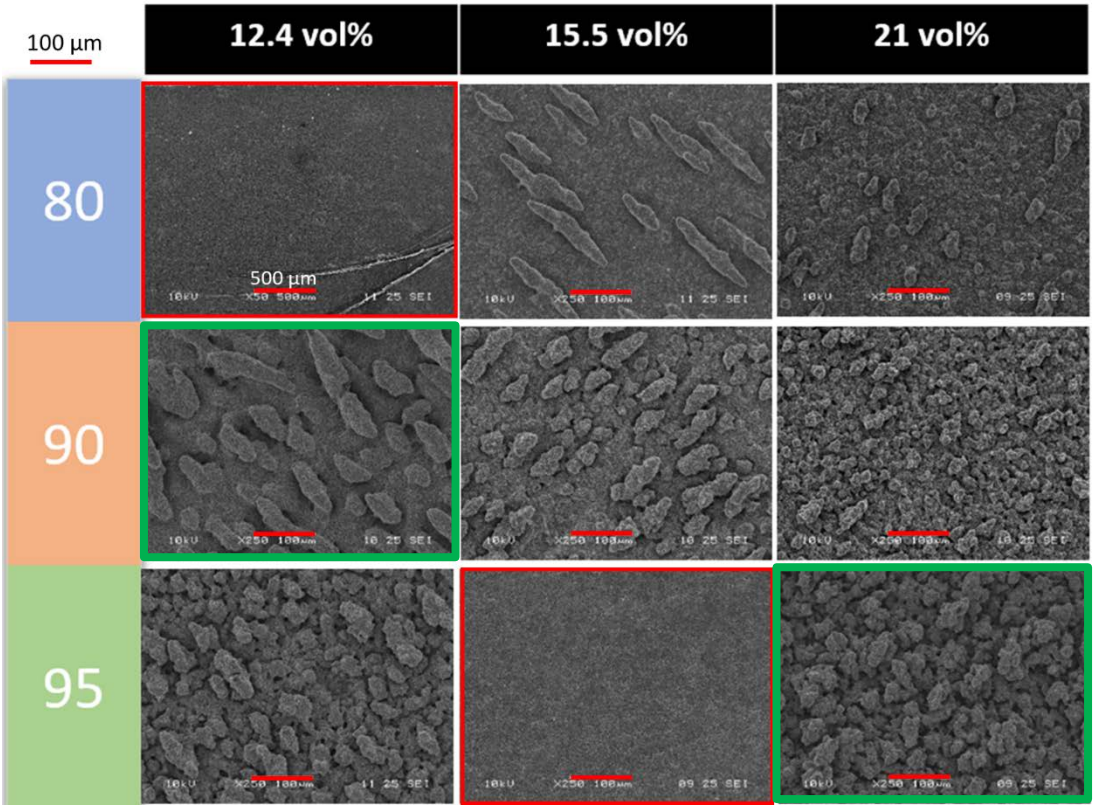

Figure 20. Top-down SEI-SEM images taken at 250x and 50x, depicting the 9 cathode tapes and the surface features created by the printing process. Each ink seems to have created a different surface morphology that will affect how the tape interacts with the electrolyte.

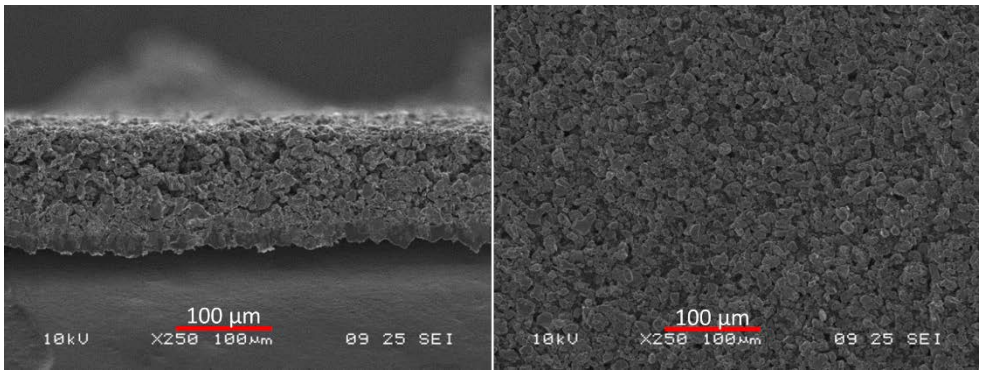

Figure 21. SEI-SEM images of the 95/2.5/25 cathode tape fabricated with the standard tape casting process. The tape cast has a relatively flat surface with some porosity throughout. The porosity does seem less connected to the surface when compared to the printed tapes and electrolyte may have trouble penetrating into the material. *Left)* Cross-sectional image at 250x. *Right)* Top-down image at 250x.

In **Figure 22** the top down view of the tapes the 90/5/5, 12.4 volume percent has smoother features while the 95/2.5/2.5, 21 volume percent appears rough. It is difficult to measure the size of the rougher features as they are convoluted with less defined edges than the smoother features. For the 80/10/10, 15.5 volume percent, the smooth features appear to be within 50 – 175 µm and are aligned in the direction the print head moves in. The 90/5/5, 12.4 volume percent tape has a higher density of these smooth features and these range from 25 – 200 µm. These features are less clearly aligned with the direction of the print head. The 80/10/10 12.4 volume percent tape has the most flat space between small features 25 – 50 µm. The other tapes, other than the outliers, have rough more convoluted surfaces.

Without reliable viscosity measurements it is difficult to determine the cause of the surface features but one theory is the cohesiveness of the ink allows these features to form. A more cohesive ink will have a tendency to be more attracted to itself than the substrate it is being printed on. The layers printed and partially dried may not attract the

sprayed ink which will not wet to the surface and instead clump. A higher viscosity, inks would be expected to be more cohesive and have more defined surface features. If the ink could be remade it would be beneficial to determine the wetting angle produced by the ink on the foil substrate as well as the wetting angle of the ink on the already printed and semi-dry cathode although this study did not have the resources to remake the ink and perform these measurements.

Table 5. Amount of printed solids, thickness and bulk density of the cathode tapes. If more solids are printed it would be expected to have a thicker tape. The tapes with the higher ratio of $LiCoO_2$ printed the thickest tapes although there was little change in bulk density between all of the tapes.

	Actual Solids Printed	Thickness	Bulk Density
	wt %	μm	g/cm^3
80/10/10, Tape cast	-	59	1.49
80/10/10, 12.4 vol%	3.1 ± 0.7	13	1.17
80/10/10, 15.5 vol%	16.0 ±1.0	54	0.94
80/10/10, 21 vol%	16.6 ± 0.9	42	0.96
90/5/5, 12.4 vol%	17.2 ± 0.5	75	1.16
90/5/5, 15.5 vol%	21.6 ± 0.8	64	1.17
90/5/5, 21 vol%	23.3 ± 1.4	63	1.03
95/2.5/2.5, 12.4 vol%	19.8 ± 0.5	88	1.10
95/2.5/2.5, 15.5 vol%	4.0 ± 1.4	13	1.87
95/2.5/2.5, 21 vol%	23.9 ± 0.5	114	1.14
95/2.5/2.5 Tape cast	-	109	2.51

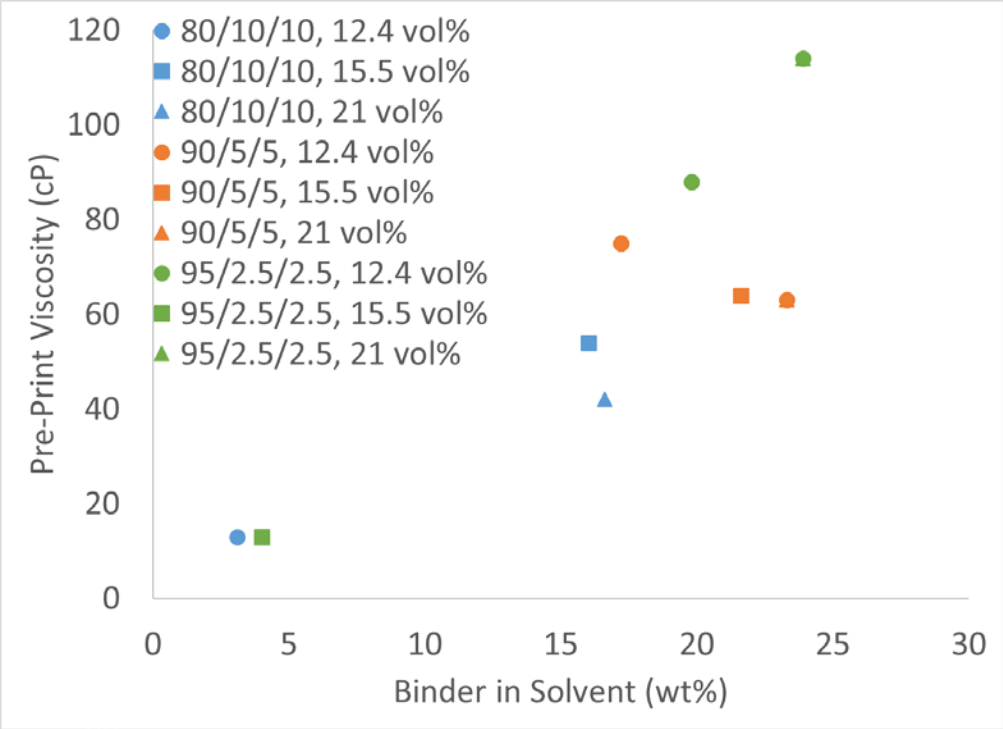

Figure 22. Effects of the amount of solids aerosolized and printed compared to physical properties of the final tape. The thickness was measured with flat-flat micrometers, after printing 50 passes. There is a general increase in thickness with increasing ratio of solids. There does not seem to be a trend with the amount of solids printed.

The bulk densities of the printed tapes were generally within 0.9 and 1.2 g/cm^3 with one exception for the very thin 95/2.5/2.5, 15.5 volume percent tape. This density of the tape was higher due to the lack of surface features as seen in **Figure 20**. This is also true for the tape cast tapes. Each tape has a density significantly higher than its printed counterparts, when considering the same ratio of materials. For the rest of the printed tapes, if at least 90% of the solids in the ink are aerosolizing, the densities are pretty consistent for these print conditions, regardless of the ink composition. This indicates the surface features are building in a way that keeps the density constant regardless of the ink composition, while the thickness is changing drastically.

The raised surface features achieved through printing could be beneficial to the electrochemical performance and specific capacity. These features would allow for more surface area to be available to the electrolyte if it is able to access and flow around these features. The electrochemical testing will examine whether these features show an improvement.

Weight Loss Study

The weight loss study estimates the actual ratio of $LiCoO_2$ in the final tape. This is achieved by oxidizing the binder and carbon so only the lithium cobalt oxide remains as shown in **Figure 13** on the tape cast cathode. There are two distinct drops in weight below 600°C that are attributed to the binder and carbon. Determining the actual weight of the binder and carbon using this method is difficult as there is overlap in the temperatures at which these components oxidize. The measurement of $LiCoO_2$ is taken directly after the second drop from each deposition sample, and these values are then averaged. The TGA data from one of the deposition samples from each tape is plotted in **Figure 23**. One feature of note is above 800°C there is another smaller drop that corresponds to a decomposition of the $LiCoO_2$. This drop is not apparent in the as-received powder or the tape cast cathode and is believed to occur in the printed tapes due to the particle size reduction. A smaller particle is typically more reactive, allowing it to oxidize more readily. The increased reactivity may be beneficial as it could help the $LiCoO_2$ give up the lithium ions more readily than larger particles that must diffuse the material through a greater mass before reaching the electrolyte. On the other hand, if the material reacts more readily with the electrolyte it can form unwanted products.

The new ratios of active material in the printed solids as seen in **Table 6** were calculated by averaging the weights taken from a sampling of deposition samples, at approximately the red line shown in **Figure 23**. This is only an estimate of the amount of material contained in the printed tape however it is believed to be a better estimation than the initial ratio used for the ink.

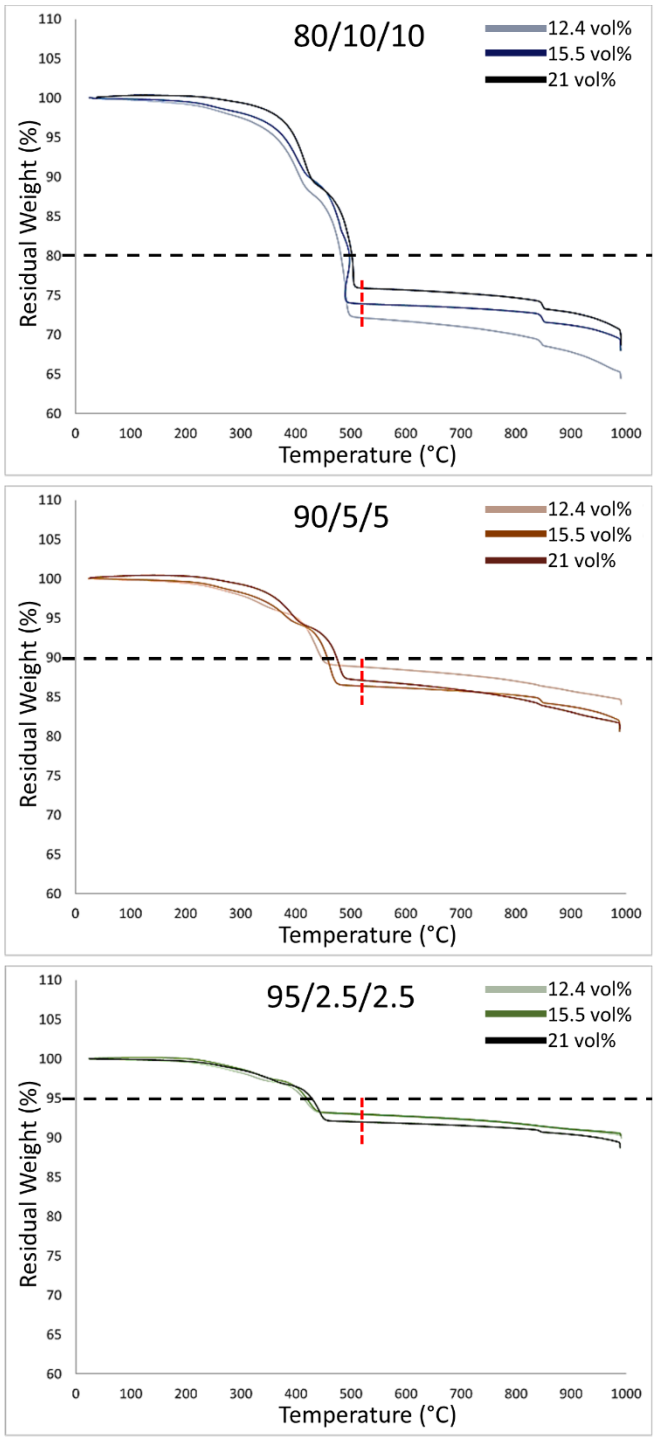

Figure 23. TGA weight loss of deposition rate samples tested from room temperature to 1000°C. There are two primary weight loss drops for the binder and carbon and a smaller drop above 800°C indicating the active material is oxidizing. This drop is more apparent in some samples than others which may indicate some samples smaller particles of $LiCoO_2$.

Table 6. TGA results of the residual weight percentages of $LiCoO_2$ in the printed tapes. The ratio of $LiCoO_2$ is lower in every printed tape than the ratio originally in the ink. The loss of material is expected to occur during the printing process and is not observed in the tape cast batteries.

Expected	12.4 vol%	15.5 vol%	21 vol%
80%	63.1 ± 11	72.2 ± 1.7	73.4 ± 2.3
90%	87.8 ± 1.1	86.1 ± 0.4	84.3 ± 2.7
95%	93.2 ± 0.1	89.1 ± 6.9	91.1± 0.9

In each case the amount of $LiCoO_2$ was lower than what was originally put into the ink, noted in the expected column of **Table 6** and by the black lines in **Figure 23**. The 80/10/10 ink seemed to have the largest reduction in expected LCO. The 80/10/10 tapes saw the largest $LiCoO_2$ reduction and highest spread, 6-17%, and the 90/5/5 and 95/2.5/2.5 tapes both saw a 2-6% reduction. This may indicate the 80/10/10 tapes were the least stable ink configuration under these conditions. Fortunately this ratio is typically only used during research in an attempt to conserve the expensive active material. Most production level batteries prefer a higher percentage of active material in the final product.

Unexpectedly, the 95/2.5/2.5, 15.5 volume percent outlier performed relatively well (6% reduction) when compared to the other outlier, 80/10/10, 12.4 volume percent tape (17% reduction). The 95/2.5/2.5, 15.5 volume percent tape was still printing near the expected ratio of solids even though the amount of solids printed was extremely low (4% solids printed). It is wasteful to leave solids behind when printing but this tape may perform better electrochemically than would be expected. Thin cathodes are useful to achieve a higher power density, where the reaction progresses more quickly to

completion than a heavier thick tape that will have a higher energy density. A thinner cathode results in a shorter distance for the ions to travel.

A lower ratio of active material in the tape could be explained by an unstable ink where the $LiCoO_2$ is settling too quickly and the binder and carbon are printing preferentially. This would be expected if there is too little binder or carbon to appropriately suspend the $LiCoO_2$ or the particles are too large and sinking to the bottom. Either scenario would indicate an unstable ink. Issues in the printer such as a clogged nozzle could also result in less $LiCoO_2$ making it into the final print.

The electrochemical testing software uses the weight of the active material in the cathode, which is calculated using the ratio of active material in the ink, to calculate the battery capacity and generate the current for the assigned charge rate. These values are calculated with equation 9.

If the ratio of active material printed is not equal to the amount put into the ink, the theoretical capacity will be lower than what is calculated and the battery will reach full charge in less time than is expected based on the assigned C rate. This problem is not seen when testing tape cast materials because 100% of the ink is used in the final product, so any decrease in the capacity is directly attributed to the electro chemical problems within the cell. With printed batteries the stability of the ink and final tape composition must also be considered.

Using the weights obtained from the TGA data presents a more representative capacity for each printed tape when the values are recalculated using the new ratios and equation 9. The capacities were calculated using both the ratio of $LiCoO_2$ in the ink and the ratios of $LiCoO_2$ in **Table 6** and the results are reported in **Table 7**. Some of the tapes

showed a significant weight change which results in a large capacity change, up to 21% for the 80/10/10, 12.4 volume percent. This $LiCoO_2$ that is not making it into the battery is left in the ink container which is not ideal due to the high cost of the material and the fact that a higher capacity battery is almost always desirable.

Table 7. The measured weight of the $LiCoO_2$ and the calculated maximum capacity using the ratio of $LiCoO_2$ in the ink and recalculated with the ratio of $LiCoO_2$ found during the weight loss study. There is a significant change in the maximum capacity which will affect the cyclic testing.

	Measured Weight	Maximum Capacity	Recalculated Maximum Capacity	Capacity Change
	g	mAh	mAh	%
80/10/10, Tape cast	0.0174	1.95	1.96	0.8
80/10/10, 12.4 vol%	0.0030	0.34	0.27	-21.1
80/10/10, 15.5 vol%	0.0101	1.13	1.02	-9.8
80/10/10, 21 vol%	0.0080	0.90	0.82	-8.3
90/5/5, 12.4 vol%	0.0172	2.17	2.11	-2.5
90/5/5, 15.5 vol%	0.0148	1.86	1.78	-4.3
90/5/5, 21 vol%	0.0096	1.21	1.13	-6.4
95/2.5/2.5, 12.4 vol%	0.0192	2.55	2.50	-1.9
95/2.5/2.5, 15.5 vol%	0.0048	0.64	0.60	-6.2
95/2.5/2.5, 21 vol%	0.0258	3.43	3.29	-4.1
95/2.5/2.5 Tape cast	0.0541	7.20	7.20	0.0

As is expected the 95/2.5/2.5 tape cast battery has the highest capacity, due to its greater bulk density. The low thickness of the 80/10/10 tape cast battery allowed the 3

thickest printed batteries to have a higher capacity than this tape cast battery, however if this was recast closer to 100 μm this would not be the case based on the bulk density of this cathode. A more energy dense battery is typically preferred to maximize the total output the battery is capable of but this may sacrifice power density and result in poor performance at higher charge rates. The surface morphology of the printed batteries may reduce the reduction seen in the thicker, denser batteries as the charge rate is increased.

It is important to note these capacity values are far lower than the amount of energy typically found in our car batteries 50 mAh or cell phone batteries 2500-4000 mAh, and for reference should be compared to each other or the tape cast batteries. The production level batteries create stacks of the material or very thick electrodes to ensure higher capacity values.

Electrochemical Testing

If the discharge, C, rate increases there is expected to be some decrease in the capacity because the reaction will have less time to complete. The batteries were cycled at a variety of discharge rates as is common practice in the laboratory and can be seen in **Figure 24**. The first cycle of the two batteries tested for each composition were averaged to determine a maximum capacity value and the last 25 cycles were averaged to determine the reduction in capacity after 50 cycles and these values are also graphed in **Figure 25** and recoded in **Table 8**. If the first cycle is above that of the tape cast battery and the printed batteries maintain 80% of the theoretical maximum capacity (recalculated using TGA adjusted $LiCoO_2$ weights) over all 50 cycles then the batteries are considered passable.

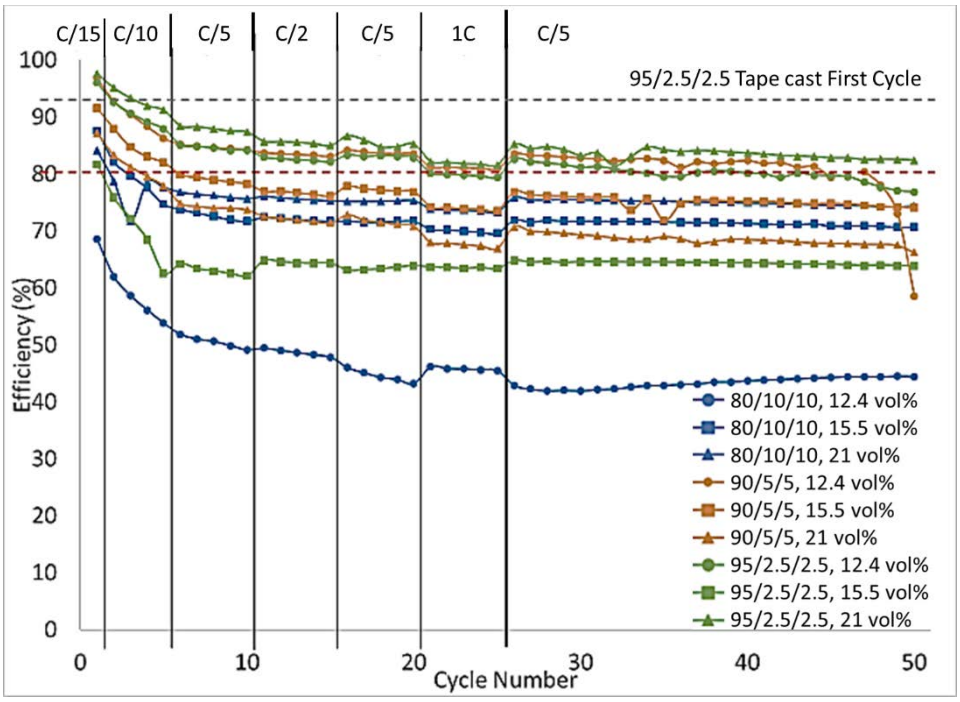

Figure 24. Average capacity from cyclic testing of two batteries. The reduction over time and decrease in capacity as rate increases are both observed in this chart.

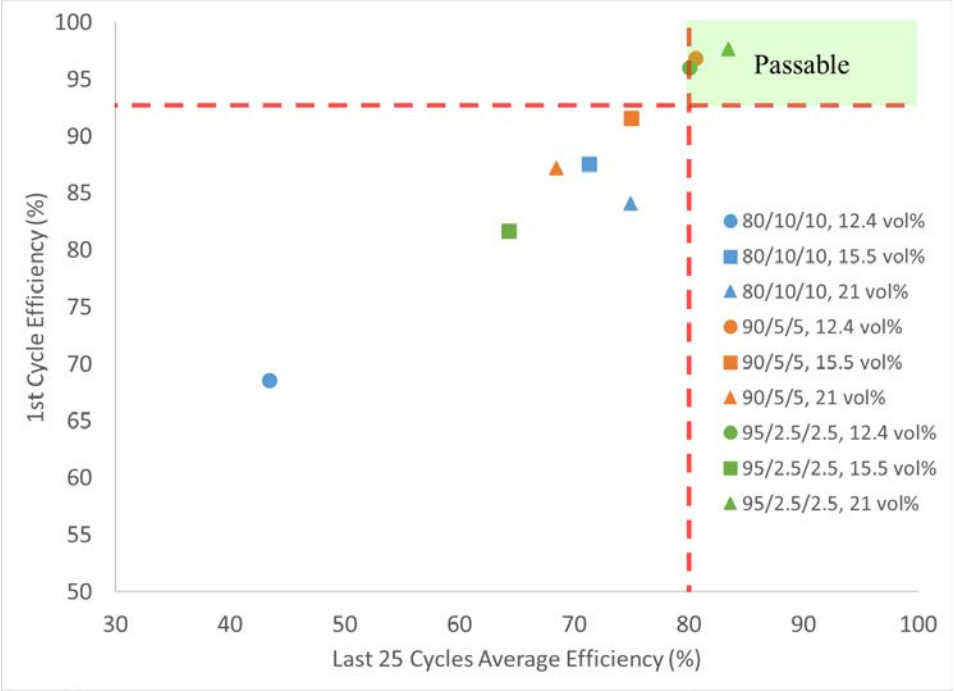

Figure 25. The relationship of the first cycle, maximum capacity, and the average capacity of the last 25 cycles is depicted in this graph. The 3 batteries can be considered viable when compared to similar tape cast batteries.

Table 8. The data from the average of the two batteries tested at cycle 1 at C/15 rate and the capacities averaged over the last 25 cycles at C/5 rate. Ideally the tapes will have a larger 1st cycle capacity than the tape cast and a reduction greater than 80% of the theoretical capacity or 112 mAh/g.

	Cycle 1, C/15 Rate		Cycle 25-50, C/5 Rate	
	Recorded Capacity	Specific Capacity	Recorded Capacity	Specific Capcity
	mAh	mAh/g	mAh	mAh/g
80/10/10, Tape cast	1.775	126.6	-	-
80/10/10, 12.4 vol%	0.182	96.0	0.115	60.8
80/10/10, 15.5 vol%	0.894	122.6	0.728	99.8
80/10/10, 21 vol%	0.691	117.7	0.616	104.9
90/5/5, 12.4 vol%	2.046	**135.6**	1.703	**112.8**
90/5/5, 15.5 vol%	1.635	128.2	1.339	105.0
90/5/5, 21 vol%	0.988	122.1	0.775	95.8
95/2.5/2.5, 12.4 vol%	2.404	**134.4**	2.004	**112.1**
95/2.5/2.5, 15.5 vol%	0.489	114.4	0.385	90.0
95/2.5/2.5, 21 vol%	3.213	**136.7**	2.745	**116.8**
95/2.5/2.5 Tape cast	6.670	129.8	-	-

The batteries with the thickest printed cathodes 95/2.5/2.5, 12.4 and 21 volume percent, and 90/5/5, 12.4 volume percent had a higher specific capacity than the 95/2.5/2.5 tape cast batteries and maintained 80% capacity over all 50 cycles. Referring back to **Figure 19** these cathodes appeared to have the most interconnected porosity which would allow more contact between the cathode and electrolyte. These three tapes had relatively different shaped features on the surface and a $LiCoO_2$ reduction of between

1.8 and 3.9 % when compared to the ink. These 3 batteries provide evidence to say our first objective was met and this printing method could be used in place of the tape casting method when the ink is tailored properly for the printing conditions.

The other ink compositions did not meet the set requirements however there are some interesting electrochemical characteristics that can be related to the physical characteristics of the tapes. As the rate is increased the efficiency of the battery is expected to decrease as is shown in **Figure 26** for cycles 16-30 where the rate changes from 0.2C to 1C and back to 0.2C. With a higher power density the battery will be able to perform better at faster rates and the decrease in efficiency will be less apparent. The change in efficiency for the batteries is recorded in **Table 9**. The very thin 95/2.5/2.5, 15.5 volume percent battery with no surface morphology had a very small decrease in efficiency, 0.2%, when the rate was increased from 0.2C to 1C. This occurs in very thin cathodes, the lithium is able to quickly migrate from the cathode even when the rate is increased but is accompanied by a lower capacity and poor energy density as is also the case with this battery. The change in efficiency has a linear relationship to the thickness of the battery as shown in **Figure 27**. The thinner the battery the higher the power density but the lower the capacity.

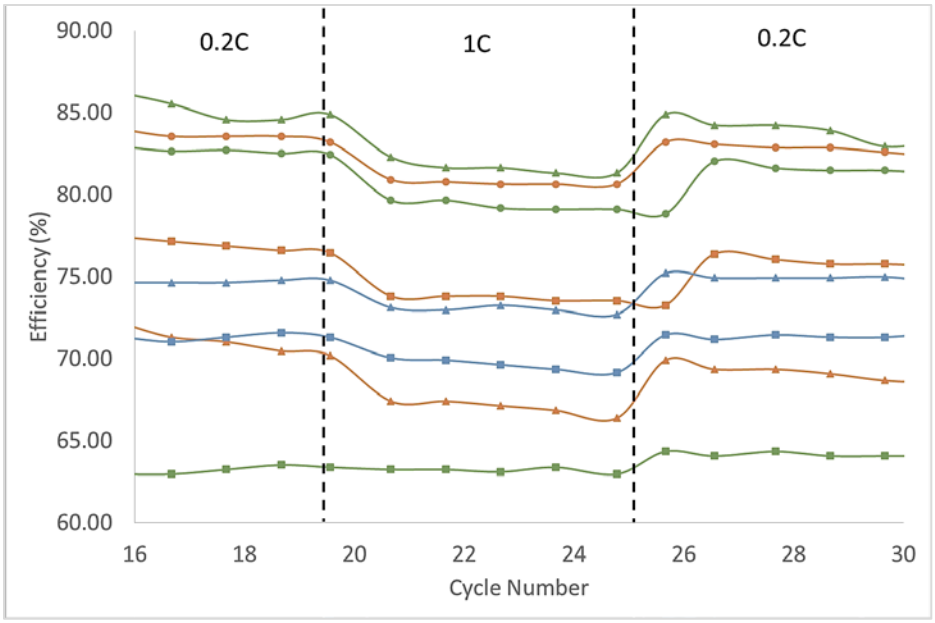

Figure 26. An increase in the discharging rate is accompanied by a decrease in the efficiency of the battery. This changes was smaller in the thinner battery which is believed to have a higher power density.

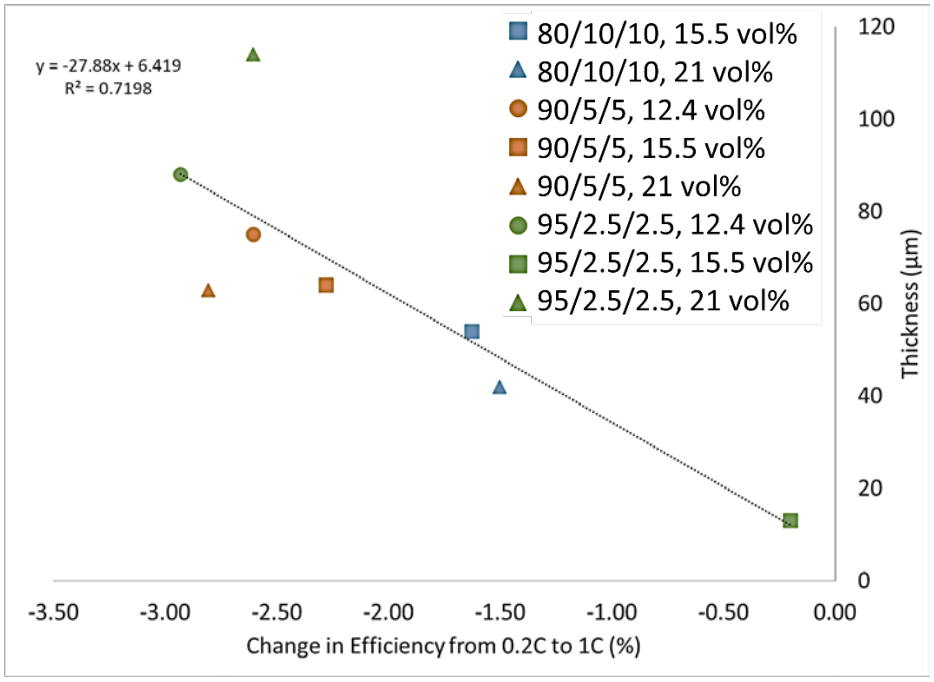

Figure 27. The change in efficiency as the charge rate is increased is linearly related to the thickness of the battery.

Table 9. The change in the efficiency as the discharge rate is changed from 0.2C to 1C. A smaller change in efficiency typically relates to a higher power density for the battery.

	Change in efficiency as charge rate is increased (%)	Change in efficiency as charge rate is decreased (%)
80/10/10, 15.5 vol%	-1.63	2.6
80/10/10, 21 vol%	-1.50	2.6
90/5/5, 12.4 vol%	-2.61	3.3
90/5/5, 15.5 vol%	-2.28	3.6
90/5/5, 21 vol%	-2.81	3.7
95/2.5/2.5, 12.4 vol%	-2.93	3.3
95/2.5/2.5, 15.5 vol%	-0.20	1.4
95/2.5/2.5, 21 vol%	-2.61	3.6

The resistance of the battery provides a good indication of how the chemical reaction is progressing. The Nyquist plots created through EIS after cycling the battery 3 times are graphed in **Figure 28** and the resistance values obtained from these plots are listed in **Table 10**. The majority of the batteries had both lower ohmic and charge transfer resistances when compared to the tape cast battery. This indicates the mixing and printing process for printing does not add elements, such as hydrates or contaminants, which increase the resistance of the printed tape. The resistances has a linear relationship to the specific capacity of the batteries. As the specific capacity decreases the resistance increases as is shown in **Figure 29**.

Table 10. The ohmic and charge transfer resistances of the battery can be determined from the Nyquist plots. The majority of the batteries had lower resistance than the tape cast battery, indicating the printing process does not have a negative effect on the final product.

	Ohmic Resistance (Ohms)	Charge Transfer Resistance (Ohms)
80/10/10, 12.4 vol%	10.4	200
80/10/10, 15.5 vol%	30.8	102
80/10/10, 21 vol%	11.6	64
90/5/5, 12.4 vol%	8.1	36
90/5/5. 21 vol%	8.7	60
95/2.5/2.5, 12.4 vol%	13.0	48
95/2.5/2.5, 15.5 vol%	8.1	119
95/2.5/2.5, 21 vol%	9.8	49
95/2.5/2.5 Tapecast	22.2	112

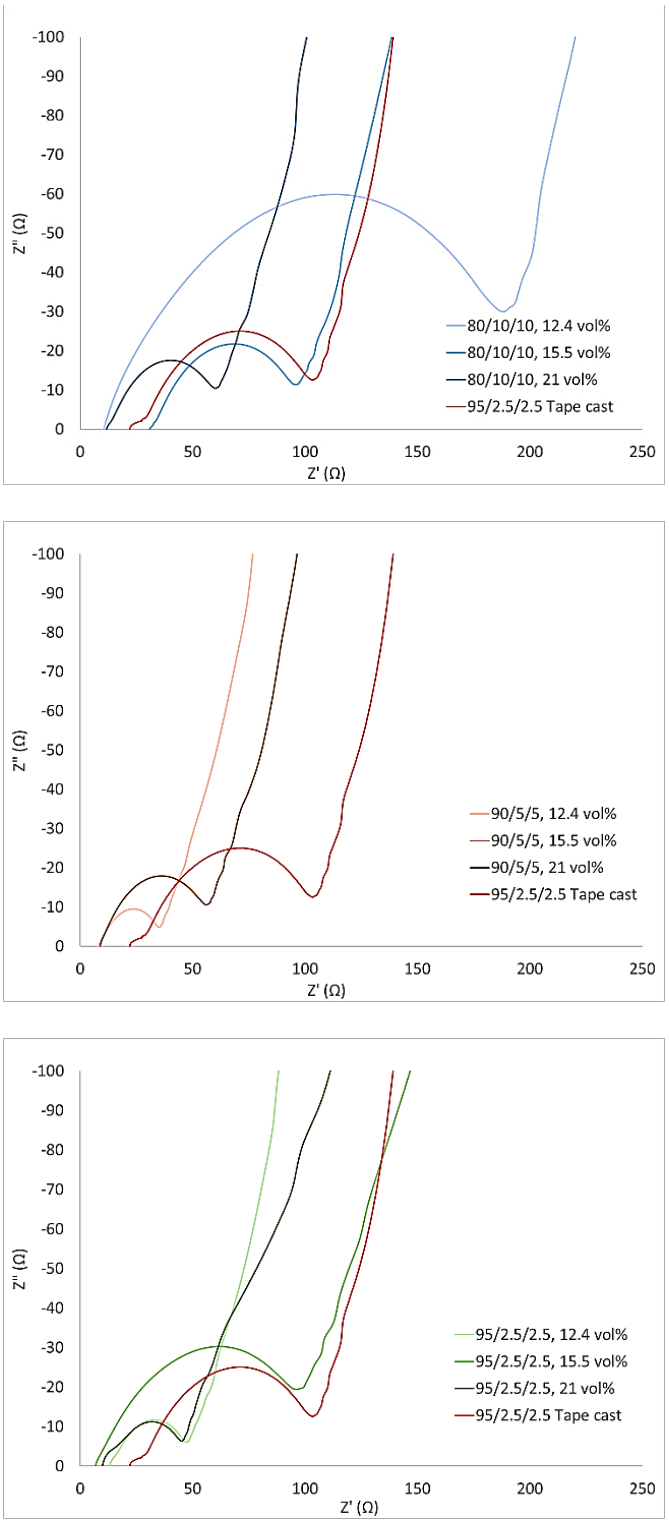

Figure 28. Nyquist plots performed with an AC voltage of 10 mV from 1 Hz to 1 MHz. Lower resistance batteries relate to better performance and higher measured capacity.

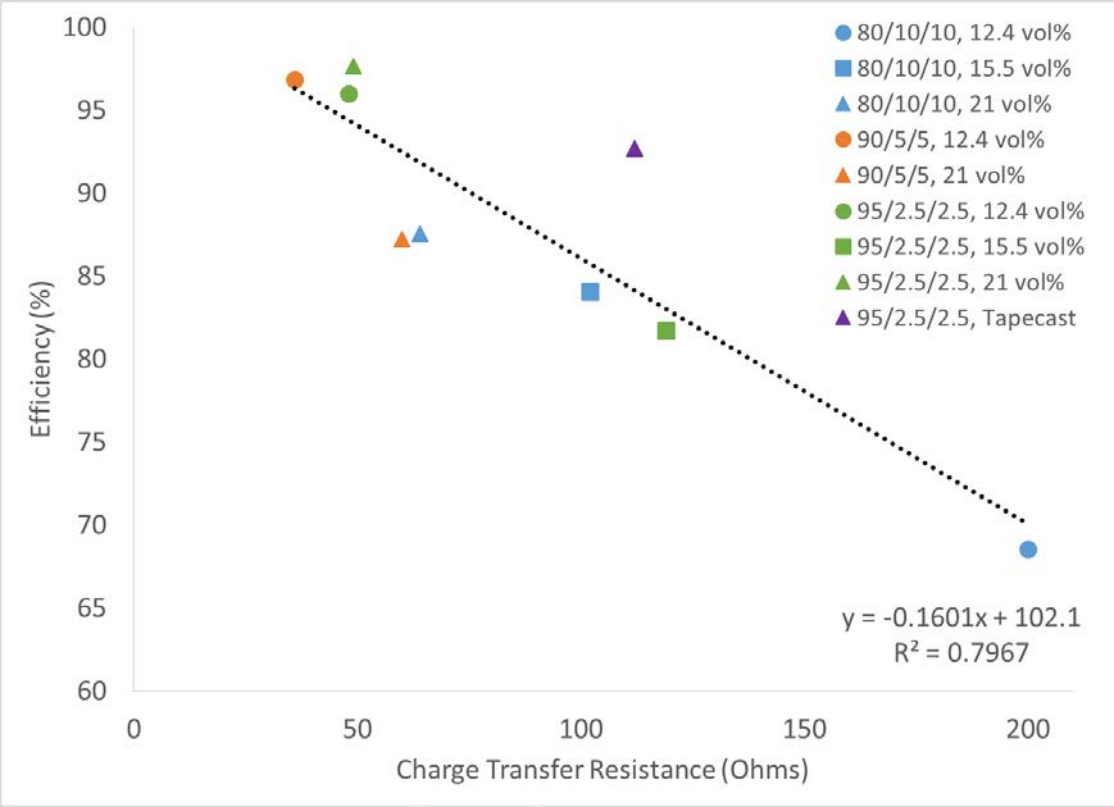

Figure 29. As the charge transfer resistance increases the efficiency decreases.

The cyclic voltammetry shows the oxidation reactions occurring at voltages typical for $LiCoO_2$ cathodes. If these reactions are not present it may indicate the lithium is not being fully removed. Cyclic voltammetry is performed at a much slower C rate than most batteries are actually used for. If the reactions are not taking place in this time frame than the battery will not be considered passable. The primary output for this data is current density. The more active material in the battery the higher the current density is expected to be. The cyclic voltammetry plots are graphed in **Figure 30**.

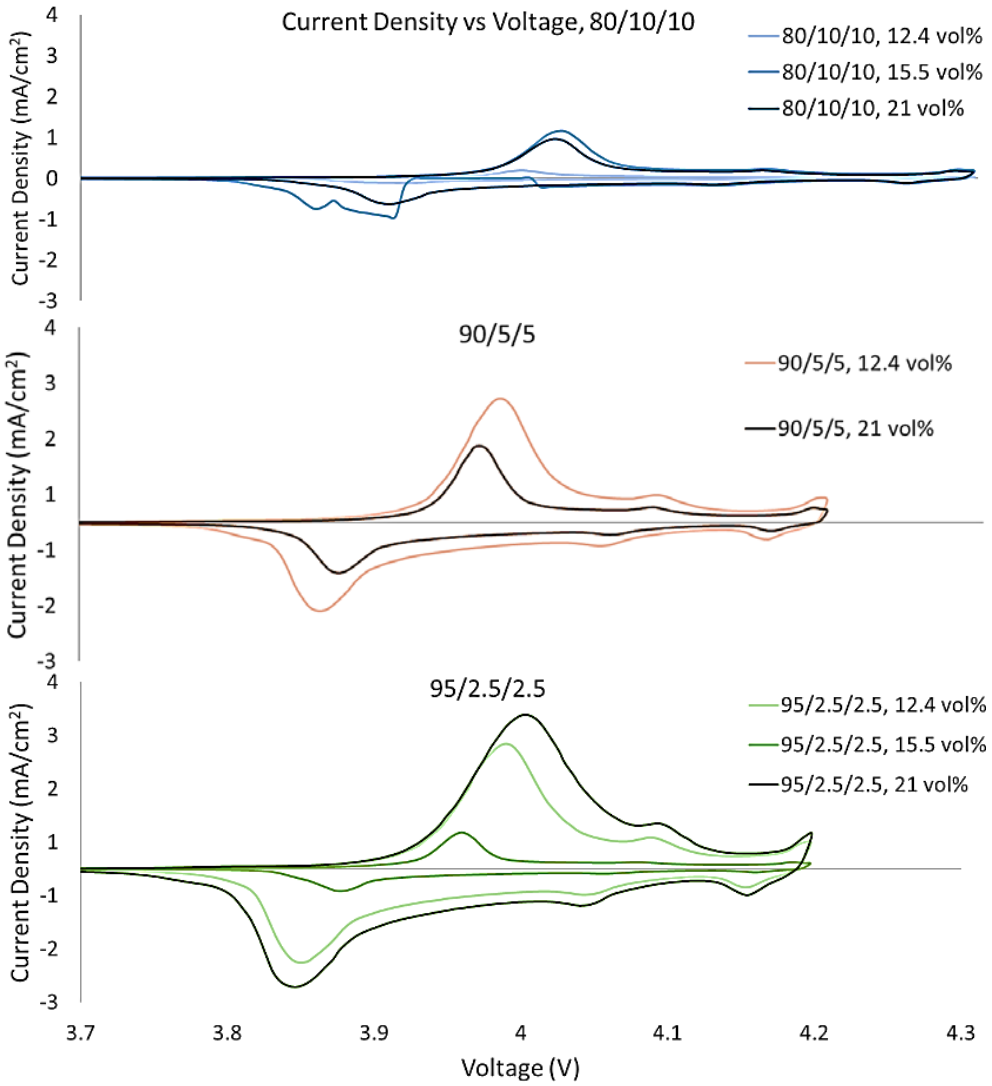

Figure 30. Cyclic voltammetry, the largest peak in the cathodic and anodic traces indicates a change in oxidation state for the Co^{4+}. The smaller peaks at higher voltages relate to phase transformations in the $LiCoO_2$.

V. Conclusions and Recommendations

Conclusions of Research

The first objective, to print a $LiCoO_2$ cathode that performed as well if not better than a tape cast cathode, was met. Three of the printed cathodes obtained a maximum specific capacity that surpassed the 95/2.5/2.5 tape cast battery and maintained 80% of the theoretical capacity through all 50 cycles. The second objective to determine the effect of ink composition on the surface morphology of the tape is inconclusive. Each composition resulted in a different morphology, shown with the top down and cross sectional SEM images, however the ink characterization techniques utilized were inadequate.

All batteries had a lower calculated maximum capacity (0.27-3.29 mAh) than the tape cast battery (7.20 mAh) and were less energy dense as a result. The surface features on the printed batteries resulted in a lower bulk density (0.94-1.87 gcm^{-3}) than the bulk density of the 95/2.5/2.5 tape cast battery (2.51 gcm^{-3}). The surface features that appeared as a result of the printing process were a direct cause of this lower density. The printed material clumped into different features rather than creating a solid dense tape except for the 80/10/10, 12.4 vol% and 95/2.5/2.5, 15.5 vol%. Neither of these tapes exhibited surface features and both had a low ratio of solids to solvent printed resulting in 13 μm thick tapes. Neither of these tapes performed well in terms of specific capacity but the ability to recover after increasing the charge rate was improved significantly in the 95/2.5/2.5 15.5 volume percent tape. The 95/2.5/2.5, 15.5 volume percent tape proved to

be the densest printed tape. These results indicate this tape had a higher power density even though the energy density was very low.

The tapes with surface features had specific capacities between 136.7 – 117.7 mAh/g which can be compared to the specific capacity of the 95/2.5/2.5 and 80/10/10 tape casts batteries, 129.8 and 126.6 mAh/g respectively. The 95/2.5/2.5, 12.4 and 21 volume percent and the 90/5/5, 12.4 volume percent printed cathodes surpassed the performance of the tape cast cathodes. The increase in specific capacity performance indicates the active material in these printed cathodes is more accessible than the material in the denser tape cast cathodes. SEM images show interconnected porosity running through the thickness of the cathodes that can be infiltrated with electrolyte providing a path for lithium ions to travel.

These features also seem to have a benefit on the electrode resistance in the battery. Both the ohmic and charge transfer resistances in the printed tapes, with surface features, was lower than that of the tape cast cathodes. This indicates the lithium ions were able to migrate more easily between the electrodes.

For most of the cathode, the reduction in particle size, achieved through ball milling, allowed the $LiCoO_2$ to remain suspended so the printed material resembled the same composition as the ink. In each ink there was some decrease in both the amount of solids printed and the ratio of $LiCoO_2$, as compared to the ink composition. The particle size reduction allowed the $LiCoO_2$ material to print however the ink was still difficult to stabilize in some cases leading to two cathodes with less than 5% of the solids printed. In addition a reduction of 2-17% $LiCoO_2$ compared to additives was found in each of the tapes. The $LiCoO_2$ that did not end up in the print is considered waste. This lack of ink

stability also led to unreliable viscosity measurements. This reinforces the need to tailor the ink to the printing and mixing conditions. Holding these variables constant allowed us to directly compare the effect the composition had on surface morphology however the prints could be improved by remaking the inks with different mixing and printing conditions.

The conditions chosen were ideal for the 95/2.5/2.5, 12.4 and 21 volume percent and the 90/5/5, 12.4 volume inks which produced high performing cathodes when compared to the tape cast with little wasted material. The interconnected porosity formed with these inks allowed for high specific capacity and good efficiency. This research was conducted on a very small sample size and further testing should be performed to statistically confirm these results.

Significance of Research

The ability to achieve a successful printed battery indicates the viability of this printing method. The effects caused by the surface features may be similar to the 3D printed nano-architectures created in previous work. This printing method may present an alternative method to achieving that desired microstructure. Many, thin layers of this printed battery should be able to achieve capacities similar to the tape cast battery. The porosity and surface features achieved with this method of fabrication allows access to active material that may be cut off in a denser cathode. This allows the battery to achieve higher specific capacities and be more efficient. To achieve results comparable to tape cast batteries, alternative characterization methods were required, such as the weight loss study.

Recommendations for Action

Repetition of the printing and testing is required to verify results and ensure the variability can be minimized. Valuable information was obtained by varying ink composition however future work could focus on creating stable inks for the desired composition. This will limit the amount of material left in the ink and lengthen the time it can be printed with. Limiting the amount of waste is essential when considering the rising cost of $LiCoO_2$. This may be achieved by adjusting the printing conditions as well including, plate temperature and aerosolizing pressure. A well-tailored ink will also reduce the amount of verification that must be performed to ensure proper printing. In theory a stable ink will print 100% of the solids.

Techniques should be utilized to better characterize the inks and tapes. Larger batches of ink could be created to ensure enough ink is available to print and perform a full viscosity and settling study. Determining cohesion within the ink could help us understand why the surface features are forming on the printed batteries. The surface features could then be characterized through a non-contact method such as laser profilometry.

Recommendations for Future Research

Printing on curved or 3d structures, such as a conductive mesh, could provide an opportunity to create structurally capable batteries. This spray technique could allow for good coverage of unique features allowing batteries to take on shapes other than the flat sheets the industry is accustomed to.

Printing of a gel or solid-state electrolyte and anode materials using the aerosol jet printing method would limit the steps required to fabricate the battery by allowing the active materials to be printed from a single machine, directly on top of each other. The effects of integrating the electrolyte layer into the cathode layer, by either spraying both materials at the same time or one directly on top of the other could be investigated by utilizing aerosol jet printing.

References

[1] L. J. Deiner, T. Jenkins, A. Powell and M. Rottmayer, "High Capacity Rate Capacble Aerosol Jet Printed Li-Ion Battery Cathode," *Advanced Engineering Materials,* 2018.

[2] S. Fletcher, Bottled Lightning: Superbatteries, Electric Cars, and the New Lithium Economy., Farrar, Straus and Giroux, 2011.

[3] G. E. Blomgren, "The Development and Future of Lithium Ion Batteries," *Journal of The Electrochemical Society, 164,* pp. A5019-A5025, 2017.

[4] A. M. Gaikwad, A. C. Arias and D. A. Steingart, "Recent Progress on Printed Flexible Batteries: Mechanical Challenges, Printing Technologies, and Future Prospects," *Energy Technology,* vol. 3, no. 4, 2015.

[5] G. Crabtree, E. Kocs and L. Trahey, "The energy-storage frontier: Lithium-ion battereis and beyond," *Materials & Engineering: Propelling Innovation,* vol. 40, no. 12, pp. 1067-1078, 2015.

[6] Z. Yang, R. Li and Z. Deng, "A deep study of the protection of the Lithium Cobalt Oxide with polymer surface modification at 4.5 V high voltage," *Scientific Reports,* vol. 8, no. 863, 2018.

[7] D. D. Lecce, P. Andreotti, M. Boni, G. Gasparro, G. Rizzati, J.-Y. Hwang, Y.-K. Sun and J. Hassoun, "Multiwalled Carbon Nanotubes Anode in Lithium-Ion Battery with $LiCoO_2$, $Li[Ni_1/3Co_1/3Mn_1/3]O_2$ and $LiFe_1/4Mn_1/2Co_1/4PO_4$ Cathodes," *ACS Sustainable Chem. Eng.,* vol. 6, pp. 3225-3232, 2018.

[8] H. Dai, B. Jiang and X. Wei, "Impedance Characterization and Modeling of Lithium-Ion Batteries Considering the Internal Temperature Gradient.," *Energies,* vol. 11, no. 1, pp. 220-238, 2018.

[9] R. B. a. K. Tagawa, Lithium-Ion Cell Production Processes Advances in Lithium-Ion Batteries, New York: Kluwer Academic/Plunum Publishers, 2002, pp. 267-299.

[10] R. Yazami, Y. Ozawa, H. Gabrisch and B. Fultz, "Mechanism of electrochemical performance decay in $LiCoO_2$ aged at high voltage.," *Electrochimica Acta,* vol. 50, pp. 385-390, 2004.

[11] X. Dai, L. Wang, J. Xu, Y. Wang, A. Zhou and J. Li, "Improved Electrochemical Performance of $LiCoO_2$ Electrodes with ZnO Coating by Radio Frequency Magnetron Sputtering," *ACS Applide Material Interfaces,* vol. 6, no. 18, pp. 15853-15859, 2014.

[12] Z. Yang, R. Li and Z. Deng, "A deep study of the protection of Lithium Cobalt Oxide with polymer surface modification at 4.5 V high voltage," *Scientific Reports,* vol. 8, no. 863, 2018.

[13] T.-S. Wei, B. Y. Ahn, J. Grotto and J. A. Lewis, "3D Printing of Customized Li-ion batteries with Thick electrodes," *Advanced Materials,* 2018.

[14] W. J. Fergus, "Recent developments in cathode materials for lithium ion batteries," *Journal of Power Sources,* vol. 195, pp. 939-954, 2010.

[15] K. K. Fu and Y. Wang, "Graphene Oxide-Based Electrode Inks for 3D-Printed Lithium-Ion Batteries.," *Advanced Materials,* vol. 28, no. 13, pp. 2587-94, 2016.

[16] M. S. Islam and C. A. J. Fisher, "Lithium and sodium battery cathode materials: computational insights into voltage, diffusion and nanostructural properties Published by The Royal Society of Chemistry," *Chemical Society Reviews,* vol. 43, pp. 185-204, 2014.

[17] A. Bottino, G. Capannelli, S. Munari and A. Turturro, "Solubility Parameters of Poly(vinylidene fluoride)," *Journal of Polymer Science Part B: Polymer Physics,* vol. 26, pp. 785-794, 1988.

[18] A. Smith and C. Peyratout, "Cold ceramics: Low-temperature processing of ceramics for applications in composites," *Advances in Ceramic Matrix Composites,* pp. 235-263, 2014.

[19] W. Bauer and D. Notzel, "Rheological properties and stability of NMP based cathode slurries for lithium ion batteries," *Ceramics International,* no. 40, pp. 4591-4598, 2013.

[20] M. N. Rahaman, "Tape Casting," in *Ceramic Processing*, CRC Press Taylor & Francis Group, 2007, pp. 308-311.

[21] K. Sun, W. Teng-Sing, B. Y. Ahn, J. Y. Seo, S. J. Dillon and J. A. Lewis, "3D Printing of Interdigitated Li-Ion Microbattery Architectures," *Advanced Materials*, no. 25, pp. 4539-4543, 2013.

[22] N. Singh, C. Galande, A. Miranda, A. Mathkar, W. Gao, A. Leela, M. Reddy, A. Vlad and P. M. Ajayan, "Paintable Battery," *Scientific Reports*, 2012.

[23] S. H. Lee, C. Huang, C. Johnston and P. S. Grant, "Spray printing and optimization of anodes and cathodes for high performance Li-ion batteries," *Electrochimica Acta*, 2018.

[24] M. N. Rahaman, "Powder Preparation by Mechanical Methods," in *Ceramic Processing*, Boca Raton, CRC Press Taylor & Francis Group, 2007, pp. 39-46.

[25] C.-H. Doh and A. Veluchamy, "Thermo-chemical process associated with lithium cobalt oxide cathode in lithium batteries.," in *Litihium-Ion Batteries*, C. R. Park, Ed., InTech, 01, April, 2010, pp. 35-56.

[26] "Rograv or Flexography?," UFLEX, 12 April 2017. [Online]. Available: https://www.uflexltd.com/blog/rotogravure-or-flexography/. [Accessed 2019].

[27] Office of Energy Efficiency & Renewable Energy , "https://www.energy.gov/eere/vehicles/batteries," [Online].

[28] R. M. Dell and D. A. J. Rand, Understanding Batteries, Cambridge: The Royal Society of Chemistry, 2001.

[29] S. Dhameja, Electric Vehicle Battery Systems, Woburn, MA: Butterworth-Heinemann, 2002.

[30] J. Geder, H. E. Hoster, A. Jossen, J. Garche and D. Y. Yu, "Impact of active material surface area on thermal stability of lithium cobalt oxide cathode," *Journal of Power Sources*, vol. 257, pp. 286-292, 2014.

[31] A. Mishra, A. Mehta, S. Basu, S. J. Malode, N. P. Shetti, S. S. Shukla, M. N. Nadagouda and T. M. Aminabhavi, "Electrode Materials for lithium-ion batteries," *Materials Science for Energy Technologies*, pp. 182-187, 2018.

[32] J. A. Puertolas, J. F. Garcia-Garcia, F. J. Pascual, J. M. Gonzalez-Dominguez, M. T. Martinez and A. Anson-Casaos, "Dielectric behavior and electrical conductivity of PVDF filled with functionalized single-walled carbon nanotubes," *Composites Science and Technology*, vol. 152, pp. 263-274, 2017.

[33] S. K. Martha, O. Haik, E. Zinigrad, I. Exnar, T. Drezen, J. H. Miners and D. Aurbach, "On the Thermal Stability of Olivine Cathode Materials for Lithium-Ion Batteries," *Journal of the Electrochemical Society*, vol. 158, no. 10, pp. A1115-A1122, 2011.

REPORT DOCUMENTATION PAGE

Form Approved
OMB No. 074-0188

1. REPORT DATE *(DD-MM-YYYY)*	**2. REPORT TYPE**	**3. DATES COVERED** *(From – To)*
03-26-2020	Master's Thesis	Sept 2018 – March 2020

TITLE AND SUBTITLE

Effect of ink composition on the physical characteristics and performance of aerosol jet printed lithium cobalt oxide cathodes

5a. CONTRACT NUMBER

5b. GRANT NUMBER

5c. PROGRAM ELEMENT NUMBER

6. AUTHOR(S)

Powell, Amber S.

5d. PROJECT NUMBER

5e. TASK NUMBER

5f. WORK UNIT NUMBER

7. PERFORMING ORGANIZATION NAMES(S) AND ADDRESS(S)
Air Force Institute of Technology
Graduate School of Engineering and Management (AFIT/ENY)
2950 Hobson Way, Building 640
WPAFB OH 45433-8865

8. PERFORMING ORGANIZATION REPORT NUMBER

AFIT-ENP-MS-20-M-114

9. SPONSORING/MONITORING AGENCY NAME(S) AND ADDRESS(ES)
Air Force Research Laboratory - RQQE
1950 Fifth St. WPAFB, OH 45433
937-656-4647, thomas.howell.1@us.af.mil
ATTN: Thomas Howell

10. SPONSOR/MONITOR'S ACRONYM(S)

AFRL/RQQE

11. SPONSOR/MONITOR'S REPORT NUMBER(S)

12. DISTRIBUTION/AVAILABILITY STATEMENT

DISTRUBTION STATEMENT A. APPROVED FOR PUBLIC RELEASE; DISTRIBUTION UNLIMITED.

13. SUPPLEMENTARY NOTES

This material is declared a work of the U.S. Government and is not subject to copyright protection in the United States.

14. ABSTRACT

Nine ink compositions were formulated and printed utilizing aerosol jet printing to form lithium cobalt oxide battery cathodes. This fabrication method is being investigated to determine the viability and potential benefit of aerosol jet printing for unique parts where a flat dense cathode would be undesirable. The conditions for creating the ink and printing of the tapes were held constant. The inks and resulting cathode tapes were characterized utilizing TGA, SEM, and electrochemical testing to observe the effect of ink composition on the surface roughness and electrochemical properties of the cathode tapes. The printed tapes had unique surface features that seemed to be ink dependent. This resulted in less dense tapes than the tape cast cathodes. Many of the tapes had a higher specific capacity when compared to similar tape cast materials. These results show this to be a viable fabrication method for lithium cobalt oxide cathodes and further investigation would be encouraged.

15. SUBJECT TERMS

Aerosol Jet Printing, Lithium Cobalt Oxide Cathodes

16. SECURITY CLASSIFICATION OF:			**17. LIMITATION OF ABSTRACT**	**18. NUMBER OF PAGES**	**19a. NAME OF RESPONSIBLE PERSON**
a. REPORT	**b. ABSTRACT**	**c. THIS PAGE**			Maj Nicholas Herr, AFIT/ENP
U	**U**	**U**	**UU**	110	**19b. TELEPHONE NUMBER** *(Include area code)* (937) 255-3636 x4524 nicholas.herr.1@us.af.mil

Standard Form 298 (Rev. 8-98)
Prescribed by ANSI Std. Z39-18